The transcriptional repressor Bcl6 promotes pre-TCR induced differentiation to CD4+CD8+ thymocyte and attenuates Notch1 activation

Anisha Solanki[1]*, Diana C. Yánez[1]*, Ching-In Lau[1], Jasmine Rowell[1], Alessandro Barbarulo[1], Susan Ross[1], Hemant Sahni[1] and Tessa Crompton[1,2]

[1]UCL Great Ormond Street Institute of Child Health, 30 Guilford Street, London WC1N 1EH, UK;

*Equal contribution

[2]**Correspondence:** Tessa Crompton, UCL GOS Institute of Child Health, 30 Guilford Street, London WC1N 1EH, United Kingdom. Email: t.crompton@ucl.ac.uk, Tel +44 20 7905 2893, Fax +44 20 7905 2882.

ORCHID ID: https://orcid.org/0000-0002-8973-4021

Conflict of interest statement: The authors have declared that no conflict of interest exists

Summary Statement

Here we show that Bcl6 is required for pre-TCR induced differentiation from CD4-CD8- double negative to CD4+CD8+ double positive cell in the thymus and that Bcl6 attenuates Notch1 signalling after β-selection.

Abstract

Pre-TCR signal transduction is required for developing thymocytes to differentiate from CD4-CD8- double negative (DN) to CD4+CD8+ double positive (DP) cell. Notch signalling is required for T-cell fate specification and must be maintained throughout β-selection, but inappropriate Notch activation in DN4 and DP cells is oncogenic. Here, we show that pre-TCR signalling leads to increased expression of the transcriptional repressor *Bcl6* and that Bcl6 is required for differentiation to DP. Conditional deletion of Bcl6 from thymocytes reduced pre-TCR-induced differentiation to DP cell, disrupted expansion and enrichment of icTCRβ+ cells within the DN population and increased DN4 cell death. It also increased Notch1 activation and Notch-mediated transcription in the DP population. Thus, Bcl6 is required in thymocyte development for efficient differentiation from DN3 to DP cell and to attenuate Notch1 activation in DP cells. Given the importance of inappropriate NOTCH1 signalling in T-ALL, and the involvement of Bcl6 in other types of leukaemia, this study is important to our understanding of T-ALL.

Introduction

αβT-cells develop in the thymus, which provides an essential environment for T-cell fate specification and differentiation(Koch and Radtke, 2011; Hosokawa and Rothenberg, 2018). CD4-CD8- (DN) cells differentiate via an immature CD8+ single positive (ISP) to become CD4+CD8+ (DP) cells, which give rise to CD4 or CD8 T-cells. The DN population can be subdivided by ordered expression of CD44 and CD25: CD44+CD25-(DN1); CD44+CD25+(DN2); CD44-CD25+(DN3); CD44-CD25-(DN4)(Hayday and Pennington, 2007; Shah and Zuniga-Pflucker, 2014).

Notch1 activation promotes T-cell fate in bone marrow (BM)-derived precursors entering the thymus, and mice deficient in Notch1 exhibit failed T-cell lineage commitment, while forced expression of Notch1 leads to generation of T-cells in BM(Radtke et al., 2010; Hosokawa and Rothenberg, 2018). Binding of Notch1 on lymphoid precursors with its ligand Dll4 leads to its cleavage and proteolytic release of activated intracellular Notch1 (NICD), which travels to the nucleus to bind RBPJ and coactivate transcription of target genes, including *Hes1* and *Notch3* (Reizis and Leder, 2002; Bellavia et al., 2007b). Notch signalling is maintained during β-selection (Ciofani and Zuniga-Pflucker, 2005; Hosokawa and Rothenberg, 2018), but following pre-TCR signalling, *Notch* genes are down-regulated as Id3 rises and supresses E2A-mediated transcription (Allman et al., 2001; Yashiro-Ohtani et al., 2009). Inappropriate Notch activation after β-selection is oncogenic, and contributes to T-ALL (Tzoneva and Ferrando, 2012; Pelullo et al., 2014).

The pre-TCR complex is essential for αβT-cell development to stop further recombination of the *TCR-β* loci, induce expansion and differentiation from DN3 to DP, and rescue developing T-cells from apoptosis. Several other signalling pathways are involved in this process, including IL7, Hedgehog and Wnt signalling (Staal et al., 2001; Goux et al., 2005; Outram et al., 2009; Rowbotham et al., 2009; Shah and Zuniga-Pflucker, 2014; Boudil et al., 2015; Sahni et al., 2015).

Multiple studies showed that Bcl6 is a master regulator of the T follicular helper cell lineage and germinal centre B-cell fate (Ye et al., 1997; Yu et al., 2009). *Bcl6* is also expressed in developing lymphocytes, and protects pre-B cells from apoptosis during immunoglobulin light chain rearrangement, whereas in thymocytes IL7 signalling during β-selection represses *Bcl6* expression (Heng and Painter, 2008; Duy et al., 2010; Boudil et al., 2015). We used conditional deletion of Bcl6 from thymocytes to show that Bcl6 promotes pre-TCR induced differentiation to DP cell and attenuates Notch1 activation. Thus, this study is important to our understanding of T-ALL, given the significance of dysregulated NOTCH1 in this disease.

Results

Bcl6 promotes DN to DP transition in foetal thymocytes

We previously employed a modelling approach that used transcript expression and degradation measurements to identify transcriptional targets of pre-TCR signalling, and identified *Bcl6* as a candidate gene which showed increased transcription in the first 24 hours after the pre-TCR signal (Sahni et al., 2015). *Bcl6* expression in whole-genome transcription datasets confirmed that *Bcl6* is upregulated between DN3 and DP populations (Figure S1A-B).

Therefore, to investigate the role of Bcl6 in thymocyte differentiation after pre-TCR signalling, we examined thymocyte development in conditional knockout mice in which floxed *Bcl6* alleles were deleted from thymocytes from the DN2 stage onwards in thymocytes, by Cre under control of the *lck*-promotor (Bcl6f/f-lckCre+=Bcl6coKO). In these mice, LoxP sites were inserted into the *Bcl6* gene locus, flanking exons 7–9 encoding the zinc finger domain of Bcl6 (Hollister et al., 2013).

In embryos, αβT-cell development first occurs in a synchronised wave facilitating investigation of the rate of differentiation. We compared T-cell development from Bcl6coKO and control (Cre-) littermate thymus between E15.5 and E17.5, as TCRβ expression first occurs and the pre-TCR signals for differentiation to DP cell. On E15.5, the Bcl6coKO contained more thymocytes than control, and although there were no differences in the distribution of the DN subsets, the proportion of DN3 and DN4 cells that expressed intracellular (ic) TCRβ were higher in Bcl6coKO than control (Figure 1A-D). In contrast, on E16.5, the day on which the DP population first emerges, the Bcl6coKO thymus contained fewer cells than control (Figure 1E), and there was a reduction in the DP population, from 12.8% in control to 4.85% in Bcl6coKO. The CD8+ISP population was reduced from 16.6% in control to 12.0% in Bcl6coKO, whereas the proportion of DN cells increased (Figure 1F). Examination of the DN subsets revealed a small increase in the proportion of DN3 cells and decrease in DN4 cells (Figure 1G), and the percentage of cells that expressed icTCRβ was lower in DN3 and DN4 subsets in Bcl6coKO compared to control (Figure 1H). We did not detect a significant difference in the proportion of CD3+ icTCRβ- cells, which represent the γδ T-cell population, between Bcl6coKO and control thymus (Figure S2A-B). To assess cell cycle status we compared icCyclin B1 staining between Bcl6coKO and control. The proportion of cells that stained positive for icCyclin B1 was high in all populations,

reflecting the rapid increase in cell numbers in the foetal thymus during late gestation, but we did not observe significant differences between genotypes between DN3, DN4, ISP and DP populations (Figure S2C-D).

Expression of CD2, was lower in Bcl6coKO compared to control E16.5 thymus (Figure 1I). Comparison of the ratios of DN:ISP and ISP:DP showed an increase in both ratios in the Bcl6coKO, indicating that conditional deletion of Bcl6 affected the rate of transition from DN to ISP and rate of transition from ISP to DP (Figure 1J). The reduced transition to DP cell was present in E17.5 Bcl6coKO thymus compared to control, which contained fewer thymocytes, and a reduced proportion of DP cells and increase in DN cells (Figure 2A-C).

Bcl6 promotes differentiation to DP in a Rag-independent manner

Although *Bcl6* expression is upregulated after pre-TCR signal transduction, *Bcl6* RNA is present in DN3 cells before pre-TCR signal transduction (Figure S1A-B; (Heng and Painter, 2008; Sahni et al., 2015)), so it was possible that differentiation to DP cell was less efficient in the Bcl6coKO thymus as the result of an earlier influence of Bcl6 on $TCR\beta$ gene rearrangement or expression. To test this we crossed Bcl6coKO mice onto a Rag1-/- background (Rag1-/-Bcl6f/flck-Cre+=RagKOBcl6coKO; Rag1-/-Bcl6f/flck-Cre⁻ = RagKOBcl6control) and induced differentiation by anti-CD3 treatment in FTOC (Levelt et al., 1993). The transcriptional changes caused by anti-CD3 treatment of Rag-deficient FTOC mirror those that occur in defined thymocyte populations as they differentiate from DN3 to DP cell (Sahni et al., 2015). This experimental system thus enabled us to investigate rate of pre-TCR-induced differentiation from DN3 to DP independent of the requirement for $TCR\beta$ rearrangement, in a normal three-dimensional thymus environment, in which all other developmental cues, including IL7 and Dll4 were present at physiological levels. On anti-CD3 treatment, RagKOBcl6coKO

thymocytes differentiated less efficiently than RagKOBcl6control, indicating that Bcl6's role in differentiation to DP is RAG-independent. On day2 and day3 after anti-CD3 treatment, there was a reduction in the DP population in RagKOBcl6coKO compared to RagKOBcl6control FTOC and the ratio of ISP:DP was increased (Figure 2D-F).

Transcriptional Targets of Bcl6 activity at the DN to DP transition

During β-selection, IL7 signalling has been shown to reduce *Bcl6* expression in TCRβ+DN3 and DN4 thymocytes (Boudil et al., 2015). However, *Bcl6* rises after pre-TCR signalling for differentiation to DP (Figure S1A-B) (Heng and Painter, 2008; Sahni et al., 2015). Although β-selection, is absolutely dependent on the pre-TCR, it also involves coordinated signalling from IL7 and Notch pathways. Therefore, to investigate the function of Bcl6 in differentiation to DP cell, we assessed the transcriptional response to anti-CD3 treatment in thymocytes from RagKOBcl6coKO and RagKOBcl6control, so that developing thymocytes were induced to differentiate in a synchronised manner by pre-TCR signalling, but all other external signals (such as IL7) remained constant and were at normal levels. We carried out RNA-sequencing on facs-sorted thymocyte populations from RagKOBcl6control and RagKOBcl6coKO in absence of pre-TCR signalling, and after pre-TCR signal transduction for induction of differentiation to DP by anti-CD3 treatment. As expected, *Bcl6* expression (RPKM) in control cultures increased after pre-TCR signal transduction, and was ~7 fold higher in sorted ISP cells compared to the CD25+DN population, and ~6-fold higher again in the DP population (Figure 2G). To assess efficiency of deletion in the Bcl6coKO we also assessed *Bcl6* exons 7-9, which encode the zinc finger domain of Bcl6 and are floxed in this model (Hollister et al., 2013). Mean normalised reads of exons 7-9 were low in control and RagKOBcl6coKO in absence of pre-TCR signalling, but in control cultures,

expression increased after pre-TCR signalling in ISP and DP populations, whereas in the RagKOBcl6coKO, levels remained low in ISP, and were ~2.5 fold lower in the RagKOBcl6coKO DP dataset than control (Figure 2H).

We then analysed the RNA-sequencing datasets from facs-sorted CD25+DN cells in the absence of anti-CD3 treatment to investigate impact of Bcl6-deficiency on DN cells before pre-TCR signal transduction (Figure 2I-J). We used Principal component analysis (PCA) to explore the variability in datasets in an unbiased way. PCA separated datasets by genotype on PC1, which accounted for 62.2% of variability. As Bcl6 is a transcriptional repressor, we identified genes that were more highly expressed in the Bcl6coKO than control which contributed strongly to PC1, and so would potentially normally be repressed by Bcl6 (Figure 2I). These included known targets of transcriptional repression by Bcl6 in other tissues, such as *Stat1*, *Ifitm1*, *Ifitm3*, *Bcl2*, *Itm2b* and *Itgae* (Shaffer et al., 2000; Ci et al., 2009; Liu et al., 2016). Interestingly, the PCA also highlighted genes associated with the Notch signalling pathway and Notch target genes, such as the canonical Notch-target gene *Hes1*, and genes encoding components of the pathway, including *Adam10*, *Dlk1*, *Dtx3*, *Dtx3l*, *Nedd4l*, *Maml2*, *Agfg1* and *Mfng* (LaFoya et al., 2016; Kovall et al., 2017), which were more highly expressed when Bcl6 was deleted. Differentially expressed genes (DEG) (p<0.05) were identified using Ebayes statistics, and to distinguish DEG which are important for the function of Bcl6, we intersected the 3000 genes that contributed most to PC1 with the 1500 most significant DEG, to identify 1419 genes, shown clustered as a heat-map (Figure 2J). These DEG included Notch associated genes (*Adam10*, *Dtx3*, *Dtx3l*), known Bcl6-targets (*Bcl2*, *Ifitm1*), and Wnt- and Hh-signalling pathway components (*Dixdc1* and *Gli1*).

Next, to investigate the impact of Bcl6-deletion after pre-TCR signal transduction, we analysed the RNA sequencing datasets from facs-sorted CD8ISP and DP populations from anti-CD3-treated RagKOBcl6control and RagKOBcl6coKO FTOC after 2 days in culture. The RagKOBcl6coKO thymocytes differentiated more slowly than their RagKOBcl6control counterparts on anti-CD3 treatment (Figure 2D-F), so we used Canonical Correspondence Analysis (CCA) to compare their overall pattern of transcription to the transcriptional changes that occur during pre-TCR induced thymocyte differentiation from DN3 to DP cell (Figure 3A-B). We generated a scale from the transcriptome of undifferentiated DN3 cells to the transcriptome of thymocytes 21 hours after initiation of pre-TCR signal induction (Sahni et al., 2015) and plotted our datasets against this scale. The CCA showed that the four DP datasets had a more differentiated pattern of transcription than the ISP populations, but for each population the control datasets had a more mature transcriptional signature than their Bcl6coKO counterparts (Figure 3A). We then created a scale from the transcriptome of ISP and DP cells from Immgen (Heng and Painter, 2008), and used CCA to plot our datasets against this scale. For both populations, control datasets showed a more mature transcriptional signature than their Bcl6coKO counterparts (Figure 3B). Thus, these CCA confirmed that in the absence of Bcl6 pre-TCR induced differentiation is severely impaired, as not only were the size of the DP and ISP populations reduced, but the transcriptome of those cells that had differentiated was less mature than that of their control counterparts.

In keeping with the action of IL7 signalling to reduce *Bcl6* expression during β-selection (Boudil et al., 2015) and the rise in Bcl6 expression following pre-TCR signal transduction, expression of *Il7r* declined between CD25+DN, ISP and DP, and was not significantly different between any facs-sorted Bcl6coKO and control population (Figure 3C), whereas expression of *Bcl2*, a known Bcl6-target gene in other cell types, was significantly higher in all Bcl6coKO populations compared to their control counterparts, and declined as cells differentiated from CD25+ to ISP to DP (Figure 3D). PCA on ISP and DP datasets separated them by developmental stage on PC1, accounting for 43.3% variability, and by genotype on PC3, accounting for 9.4% of variability (Figure 3E). Then, to highlight genes in the ISP population important for the differences between control and Bcl6coKO, we intersected the 4000 genes that contributed most to PC3 with the 1800 significant DEG (p<0.05) between control and Bcl6coKO ISP datasets to identify 1712 genes, shown clustered as a heat-map (Figure 3F). The intersection highlighted genes that are Bcl6-targets in other tissues (*Ifitm3*, *Bcl2*, *Ifitm2*), and Notch-associated genes (eg. *Adam12, Myc, Il2ra*), including the signature Notch-target *Heyl*.

To investigate the influence of Bcl6 on the DP population, we intersected the 4000 genes that contributed most to PC3 with 3100 significant DEG (p<0.05) between control and Bcl6coKO DP datasets, to identify 2992 genes, shown clustered on a heat-map (Figure 3G). The intersection included maturation genes, expressed at lower levels in Bcl6coKO than control (*Cd4*, *Cd8a*, *Tcf7*, *Lat*), and genes involved in Notch signalling, which were expressed at higher levels in Bcl6coKO, suggesting increased Notch-mediated transcription.

Conditional deletion of Bcl6 increases Notch-mediated transcription

We therefore compared expression of Notch-associated DEG from DP datasets, and found increased expression of many genes upregulated by Notch signalling in the Bcl6coKO compared to control, and decreased expression of genes that are downregulated by Notch activation in thymocytes (Arenzana et al., 2015; Chen et al., 2019) (Figure 4A). Consequently, to test on a wider set of genes if conditional deletion of Bcl6 led to an overall increase in Notch-mediated transcription, we carried out CCA to compare our DP datasets to the transcriptome of control thymocytes and those with enhanced Notch1-mediated transcription (Arenzana et al., 2015). The Bcl6coKO datasets scored higher on the scale of control to active-Notch-signalling than control datasets, confirming that conditional deletion of Bcl6 led to greater Notch-mediated transcription in DP cells (Figure 4B).

To investigate if Bcl6 directly represses *Notch1*, *Notch3* or *Rbpj* we examined their expression levels in the RNA-seq datasets. In fact, expression of *Notch1* was modestly but significantly lower in the Bcl6coKO DN3 population compared to control ($p<0.05$), and as expected *Notch1* and *Notch3* were downregulated following pre-TCR signal transduction, whereas *Rbpj* expression remained constant (Figure 4C). None of these genes were more highly expressed in the Bcl6coKO ISP or DP populations compared to their control counterparts, indicating that the increase in Notch-mediated transcription observed in the Bcl6coKO DP cells was not because Bcl6 acts directly to repress *Notch1*, *Notch3* or *Rbpj*.

Bcl6 inhibits Notch activation

As several DEG highlighted by PCA encode molecules that regulate Notch signal transduction at the protein level, by facilitating cleavage and processing of Notch1 to generate the Notch intracellular domain (NICD), we hypothesized that Bcl6 attenuates Notch signalling by reducing formation of NICD. To test this, we compared quantity of NICD in control and Bcl6coKO thymocytes by Western blot (Figure 4D). Bcl6coKO thymocytes contained ~2.7-fold more NICD than control, but levels of Actin were equivalent. We then treated E16.5 Bcl6coKO and control FTOC for two days with Notch-inhibitor (γ-secretase-inhibitor) DAPT or its vehicle (DMSO) to confirm that the increased presence of NICD in Bcl6coKO thymocytes was attributable to increased processing of full-length Notch1. As expected, DMSO-treated Bcl6coKO FTOC contained more NICD than DMSO-treated control FTOC, and DAPT-treatment reduced the quantity of NICD in FTOC from both genotypes by ~2 fold (Figure 4E).

To test if Bcl6 promotes pre-TCR induced differentiation to DP cell in part by attenuation of Notch activation, we induced differentiation of RagKOBcl6coKO FTOC with anti-CD3 treatment in the presence of DAPT or vehicle (DMSO). DAPT-treatment reduced NICD by ~2-fold (Figure 4F), and also increased the rate of differentiation compared to the control cultures, with an increase in the percentage of DP cells and the DP:ISP ratio, and a reduction in the CD8ISP population (Figure 4G-H).

Bcl6 is required for survival of DN4 cells

Conditional deletion of Bcl6 on E16.5 led to a significant increase in icTCRβ⁻DN4 cells, which have been shown to die by apoptosis (Falk et al., 2001; Hager-Theodorides et al., 2007). We measured apoptosis by AnnexinV staining in thymocyte populations during embryonic development on E15.5 and E16.5. We detected no difference in proportion of AnnexinV+cells between Bcl6coKO and control DN3 and in E15.5 DN4 populations

(Figure 5A-B). However, on E16.5 apoptosis was increased in the Bcl6coKO DN4 population compared to control, indicating that Bcl6 promotes thymocyte survival after the pre-TCR dependent transition (Figure 5B). We also found increased AnnexinV staining in the foetal DP population (Figure 5C). Consistent with this, our RNA-sequencing datasets showed significantly higher expression of pro-apoptotic genes in Bcl6coKO DP cells compared to control, whereas expression of several anti-apoptotic genes were significantly lower (Figure 5D).

Bcl6 in adult T-cell development

In adult mice the Bcl6coKO thymus contained fewer cells than control littermate thymus, and although the proportion of DP and SP populations were not different, the proportion of DN cells was modestly decreased (Figure 6A-C). To assess cell cycle status we measured intracellular Cycin B1 expression, and found no significant differences in the proportion of positive cells between Bcl6coKO and control in DN3, DN4, ISP or DP populations (Figure S3A-B). In contrast, intracellular expression of Bcl2 was significantly higher in the Bcl6coKO DN3 and DP populations compared to control (Figure 6D-E). Within the DN population, the proportion of DN3 cells was increased and DN4 cells decreased (Figure 6F), suggesting that the reduction in the overall proportion of DN cells was due to loss of DN4 cells. Indeed, the number of DN3 cells was not different between Bcl6coKO thymus and control, whereas the number of DN4 cells was significantly lower (Figure 6F). This suggested that as in the embryo, the adult thymus showed decreased pre-TCR dependent differentiation, but that in adults it led to only a modest reduction in thymocyte number. In adult thymus T-cell development has reached steady-state, with accumulation of the DP population, and feedback mechanisms controlling the rate of differentiation to maintain production and size of the DP pool, so it is difficult to detect changes in the rate of differentiation which

are evident in synchronized foetal thymocyte differentiation (Outram et al., 2009; Rowbotham et al., 2009). We therefore synchronised T-cell development in adults in vivo by hydrocortisone-treatment to deplete thymocytes, allowing measurement of recovery of the DP population (Rowbotham et al., 2009). Three days after hydrocortisone-treatment, the Bcl6coKO thymus contained fewer DP cells and a lower ratio of DP:DN than control, confirming that Bcl6 promotes the transition from DN to DP cell in the recovering adult thymus before it has reached steady-state (Figure 6G).

In adult Bcl6coKO DN3 and DN4 populations icTCRβ expression was reduced compared to controls (Figure 7A-B), whereas we did not observe a significant difference in the proportion of cell surface CD3+ icTCRβ⁻ DN cells, which represent the γδ T-cell population, between Bcl6coKO and control thymus (Figure S3C-D). The reduction in the DN4 population and increase in proportion of icTCRβ⁻DN4 cells could be caused by failure of expansion of icTCRβ+ cells, by increased cell death of DN4 cells, or a combination of both. After pre-TCR signalling, DN3b (icTCRβ+) cells rapidly upregulate cell-surface transferrin receptor (CD71) to undergo a burst of proliferation. The percentage of CD71+ cells was decreased in Bcl6coKO DN3 cells compared to control (Figure 7C-D). Gating on DN3b enriched for CD71 expression, and in a representative experiment 55% of control DN3b cells were CD71+, compared to 20.5% in Bcl6coKO. As expected, cell surface CD71 expression was lower within the DN3a (icTCRβ⁻) population, with fewer CD71+ cells in Bcl6coKO than control. We detected no significant differences in the proportion of CD71+ cells in the DN4 populations (Figure 7E), whereas the proportion of CD71+ cells was reduced in Bcl6coKO CD8+ISP compared to control (Figure 7F). These data indicated that Bcl6-deficiency impacts on thymocyte development immediately after initiation of pre-TCR signal

transduction, and leads to a reduced proliferative burst of icTCRβ+DN3 cells, resulting in less efficient enrichment of icTCRβ+ cells within the DN4 population.

DN4 cells that fail to express icTCRβ upregulate CD69 and die by apoptosis(Falk et al., 2001). The Bcl6coKO DN4 population contained a higher proportion of AnnexinV+ and CD69+ cells than controls, confirming increased DN4 apoptosis in the absence of Bcl6 (Figure 7G-H).   QRT-PCR analysis of facs-sorted DN4 cells showed that expression of the survival gene *Bcl2l1* was lower in adult Bcl6coKO DN4 cells compared to control in two independent experiments (Figure 7I). Taken together, these data indicate that in adult thymus Bcl6 is important for efficient enrichment and expansion of icTCRβ+ DN cells and survival of DN4 cells.

Discussion

Here we identified two novel important functions for Bcl6 during T-cell development. We showed that Bcl6 is required for pre-TCR induced differentiation from DN3 to DP cell and for attenuation of Notch1 activation.

Conditional knockout of Bcl6 from foetal thymocytes resulted in reduced differentiation from DN to ISP and from ISP to DP cell and increased cell death in the DN4 population. The requirement for Bcl6 at this transition was RAG-independent, but Bcl6 deficiency resulted in dysregulated β-selection with an increase in TCRβ⁻DN4 cells and increased cell death within the DN4 population in foetus and adult. RNA-sequencing of ISP and DP populations showed that not only was pre-TCR induced differentiation less efficient in the Bcl6coKO, but also that the ISP and DP cells were less mature than their WT counterparts, confirming the requirement for Bcl6 in differentiation to DP cell.

Increased IL7 signalling to above physiological levels has also been shown to inhibit differentiation to DP cell, and as IL7 signalling leads to down-regulation of Bcl6, our study suggests that low Bcl6 expression may contribute to the arrest induced by increased IL7 signalling (Yu et al., 2004; Hong et al., 2012; Boudil et al., 2015).

Our study also indicated that Bcl6 functions to limit Notch activation in developing thymocytes but *Notch1* and *Notch3* (itself a *Notch1* target) were not differentially expressed between Bcl6coKO and control in the ISP and DP datasets. We therefore hypothesized that during thymocyte development, Bcl6 represses a set of genes that are involved in Notch processing and activation in order to attenuate the generation of NICD. Western blotting confirmed increased presence of NICD in Bcl6coKO thymocytes and that NICD concentrations were sensitive to γ-secretase inhibition. Although transcription of *Notch1* and *Notch3* are down-regulated following pre-TCR signalling, Notch1 and Notch3 protein will still be present in differentiating thymocytes after β-selection, but Notch signalling ceases during differentiation to DP cell (Allman et al., 2001; Hosokawa and Rothenberg, 2018). Inappropriate Notch activation in DN4 and DP populations causes oncogenesis and dysregulated T-cell development, so regulation of Notch activation is essential after β-selection. Several transcriptional mechanisms to limit Notch signalling have been described, including rapid downregulation of *Notch1* and *Notch3* transcription, and activation of *Ikaros* transcription by Notch3, as Ikaros then competes to silence Notch-target genes, such that in absence of Ikaros activity, increased Notch1 activation can arrest thymocyte differentiation at the DN3 stage (Bellavia et al., 2002; Bellavia et al., 2007a; Yashiro-Ohtani et al., 2009; Geimer Le Lay et al., 2014; Arenzana et al., 2015). Our study identifies an additional mechanism to attenuate Notch activation at the protein level, as we showed that Bcl6 represses expression of molecules required for Notch activation

thereby reducing production of NICD. Overall, this model suggests that Bcl6 acts to dampen Notch signalling and safe-guard against inappropriate Notch activation, as its deficiency led to upregulation of only a subset of Notch target genes. Activated Notch1 has been shown to regulate the PI3K/AKT pathway and promote cell survival (Gutierrez and Look, 2007; Wong et al., 2012), but despite the increase in NICD, in the absence of Bcl6 thymocyte cell death was increased, and we did not observe malignant transformation of thymocytes in our colony of Bcl6coKO mice.

During Xenopus development, BCL6 also restricts Notch signalling, inhibiting transcription of a subset of Notch-target genes to achieve cell-type-appropriate gene expression for left-right asymmetry (Sakano et al., 2010).

In different experimental systems increased levels of Notch1 activation/transcription have been described to promote differentiation beyond the DN3 stage in absence of TCRβ chain expression and/or to arrest thymocyte development at the DN3 stage (Michie et al., 2007; Dudley et al., 2009; Arenzana et al., 2015), whereas we showed that Notch-inhibition can recover differentiation to DP in Bcl6coKO FTOC. In the future it will therefore be important to investigate the extent to which the increase in NICD contributes to dysregulated development at the DN3 to DN4 stages and the partial arrest in differentiation observed when Bcl6 is conditionally deleted.

Our RNA-sequencing indicated that Bcl6 also influences expression of thousands of genes, including many known regulators of T-cell development. For example, conditional Bcl6-deficiency increased expression of the transcription factors *Klf2*, *Runx1* and *Gli1* and the Wnt pathway component *Dixdc1*, all important in T-cell development (Staal et al., 2001; Woolf et al., 2003; Carlson et al., 2006; Drakopoulou et al., 2010). Several DEG, which are subjects of transcriptional regulation by Bcl6 in other cell types have also been described to be transcriptional targets of Notch, amd are

involved in malignant transformation in leukaemias including T-ALL (*Myc*, *Il2ra*, *Ccnd2*, *Ccne1, Bcl2, Igf1r*) (Reizis and Leder, 2002; Weng et al., 2006; Shin et al., 2008; Rao et al., 2009; Medyouf et al., 2011; Ferreira et al., 2012; Witkowski et al., 2015), suggesting that Bcl6-Notch crosstalk may be significant in T-ALL.

In summary, our study demonstrates the importance of Bcl6 in T-cell development in the thymus at the transition from DN to DP cell. We showed that Bcl6 is required for attenuation of NICD and for pre-TCR induced differentiation to DP cell, and that Bcl6 promotes enrichment of icTCRβ+ DN cells and cell-survival after β-selection.

Methods

Animals

Bcl6f/f (Hollister et al., 2013), Rag1-/- and Lck-cre mice (Jackson Labs) were bred and maintained at UCL under UK regulations, and adults analysed at 4-6 weeks. Hydrocortisone treatment was as described (Hager-Theodorides et al., 2007).

FTOC

Foetal thymus organ cultures (FTOC) were as described (Lau et al., 2017), treated where stated with 1μg/ml anti-CD3ε (BD-Pharmingen, US) (Sahni et al., 2015) or 1μM DAPT (Sigma-Aldrich) dissolved in DMSO, which was added at equivalent concentrations to controls.

Western blots

Western blots were as described (Barbarulo et al., 2011) using anti-cleaved-Notch1 (clone Val1744, Cell Signaling) detected by X-Ray Film Processor (Protec); and anti-Actin (clone AC-15, Sigma-Aldrich) visualized by UVItec Gel-Documentation system and UVIband image software. Quantification of bands was carried out using Image J soft-ware and NICD levels were normalised to Actin levels.

Flow cytometry

Cell suspensions were prepared and stained as described(Hager-Theodorides et al., 2009) using directly-conjugated antibodies from eBioscience (San Diego, US) and Biolegend, (San Diego, US), acquired on C6Accuri (BD-Biosciences) or Cytoflex (BeckmanCoulter) and analysed using Flowjo10.6 (TreeStar, US). Intracellular staining was as described (Papaioannou et al., 2019). Apoptosis was measured using AnnexinV-FITC (eBioscience) and Annexin binding buffer (Biolegend, San Diego, USA) as described (Shah et al., 2004). To analyse immature thymocyte subsets, and exclude mature SP and γδ T-cell populations, we gated out cell surface CD3+ cells from ISP and DN populations in experiments shown in Figures 1F, 2B and 6D.

Quantitative reverse transcriptase PCR

DN4 (CD4-CD8-CD25-CD44-CD3-) were facs-sorted on FACSAriaIII, RNA extracted and Q-RT-PCR carried out as described (Yanez et al., 2019), using primers from Quantitec (Qiagen, Netherlands). RNA levels were relative to *Hprt*.

RNA-sequencing

RNA-sequencing by UCL Genomics on Illumina NextSeq500 was as described (Solanki et al., 2017). Data are available (GSE152944). Datasets were processed/standardized using Bioconductor package *DESeq2* to generate normalised estimates of transcript abundance. Differentially expressed genes (DEG) were determined using moderated Ebayes t-statistic ($p<0.05$) from *limma* package in Bioconductor. Principal Component Analysis used CRAN package *ade4*. Canonical Correspondence analysis (Ono et al., 2014) used CCA function of CRAN package 'vegan' as described (Solanki et al., 2018). To represent environmental variables of interest, the 2000 most significant DEG (lowest p-values, calculated by moderated eBayes adjusted for false-positives) between respective starting and ending precursor populations were used. In Figure 3A, scale was

generated from 2000 most significant DEG between time=0 and time=21 for time-course transcriptome datasets (Array-express E-MTAB-308) following pre-TCR signal transduction (Sahni et al., 2015). In Figure 3B, scale was generated using the 2000 most significant DEG between ISP and DP Immgen transcriptome datasets (GSE15907) (Heng and Painter, 2008). In Figure 4B, scale was generated using the 2000 most significant DEG between datasets from thymocytes with normal to high levels of Notch signalling (GSE67572) (Arenzana et al., 2015). Heatmaps in Figure 4A and 5D were generated using the CRAN package *Pheatmap* and *RColorBrewer*: rows were centred; unit variance scaling was applied to rows; and rows were clustered using Pearson correlation distance and average linkage.

To determine expression levels of different exons of *Bcl6*, we used the Python scripts dexseq_prepare_annotation.py from the Bioconductor DEXSeq package to prepare the genome annotation and then dexseq_count.py to generate counts of exons using the .bam alignment files as input. The exon count files were then inputted into DEXSeq which generated the normalized number of reads (expression) of each exon (Anders et al., 2012; Reyes et al., 2013).

Genotyping

DNA was extracted(Shah et al., 2004) and genotyped by PCR as described(Lau et al., 2012).

Primers:LckCre-Forward:GCGGTCTGGCAGTAAAAACTATC,

LckCre-Reverse:GTGAAACAGCATTGCTGTCACTT;

Bcl6fl-Forward:GTGTCCTGGGGTTACAGGTG;

Bcl6fl-Reverse: CCTGTCCTGCCTACCCATAG.

Statistical analysis

Unpaired two-tailed t-tests; probabilities significant: p≤ 0.05*;p≤ 0.01**; p≤0.001***. To allow comparison between litters, relative values for each genotype or treatment were calculated by dividing by mean of controls from same litter. Data represent at least three experiments.

References

Allman, D., Karnell, F. G., Punt, J. A., Bakkour, S., Xu, L., Myung, P., Koretzky, G. A., Pui, J. C., Aster, J. C. and Pear, W. S. (2001) 'Separation of Notch1 promoted lineage commitment and expansion/transformation in developing T cells', *J Exp Med* 194(1): 99-106.

Anders, S., Reyes, A. and Huber, W. (2012) 'Detecting differential usage of exons from RNA-seq data', *Genome Res* 22(10): 2008-17.

Arenzana, T. L., Schjerven, H. and Smale, S. T. (2015) 'Regulation of gene expression dynamics during developmental transitions by the Ikaros transcription factor', *Genes Dev* 29(17): 1801-16.

Barbarulo, A., Grazioli, P., Campese, A. F., Bellavia, D., Di Mario, G., Pelullo, M., Ciuffetta, A., Colantoni, S., Vacca, A., Frati, L. et al. (2011) 'Notch3 and canonical NF-kappaB signaling pathways cooperatively regulate Foxp3 transcription', *J Immunol* 186(11): 6199-206.

Bellavia, D., Campese, A. F., Checquolo, S., Balestri, A., Biondi, A., Cazzaniga, G., Lendahl, U., Fehling, H. J., Hayday, A. C., Frati, L. et al. (2002) 'Combined expression of pTalpha and Notch3 in T cell leukemia identifies the requirement of preTCR for leukemogenesis', *Proc Natl Acad Sci U S A* 99(6): 3788-93.

Bellavia, D., Mecarozzi, M., Campese, A. F., Grazioli, P., Gulino, A. and Screpanti, I. (2007a) 'Notch and Ikaros: not only converging players in T cell leukemia', *Cell Cycle* 6(22): 2730-4.

Bellavia, D., Mecarozzi, M., Campese, A. F., Grazioli, P., Talora, C., Frati, L., Gulino, A. and Screpanti, I. (2007b) 'Notch3 and the Notch3-upregulated RNA-binding protein HuD regulate Ikaros alternative splicing', *EMBO J* 26(6): 1670-80.

Boudil, A., Matei, I. R., Shih, H. Y., Bogdanoski, G., Yuan, J. S., Chang, S. G., Montpellier, B., Kowalski, P. E., Voisin, V., Bashir, S. et al. (2015) 'IL-7 coordinates proliferation, differentiation and Tcra recombination during thymocyte beta-selection', *Nat Immunol* 16(4): 397-405.

Carlson, C. M., Endrizzi, B. T., Wu, J., Ding, X., Weinreich, M. A., Walsh, E. R., Wani, M. A., Lingrel, J. B., Hogquist, K. A. and Jameson, S. C. (2006) 'Kruppel-like factor 2 regulates thymocyte and T-cell migration', *Nature* 442(7100): 299-302.

Chen, E. L. Y., Thompson, P. K. and Zuniga-Pflucker, J. C. (2019) 'RBPJ-dependent Notch signaling initiates the T cell program in a subset of thymus-seeding progenitors', *Nat Immunol* 20(11): 1456-1468.

Ci, W., Polo, J. M., Cerchietti, L., Shaknovich, R., Wang, L., Yang, S. N., Ye, K., Farinha, P., Horsman, D. E., Gascoyne, R. D. et al. (2009) 'The BCL6 transcriptional program features repression of multiple oncogenes in primary B cells and is deregulated in DLBCL', *Blood* 113(22): 5536-48.

Ciofani, M. and Zuniga-Pflucker, J. C. (2005) 'Notch promotes survival of pre-T cells at the beta-selection checkpoint by regulating cellular metabolism', *Nat Immunol* 6(9): 881-8.

Drakopoulou, E., Outram, S. V., Rowbotham, N. J., Ross, S. E., Furmanski, A. L., Saldana, J. I., Hager-Theodorides, A. L. and Crompton, T. (2010) 'Non-redundant role for the transcription factor Gli1 at multiple stages of thymocyte development', *Cell Cycle* 9(20): 4144-52.

Dudley, D. D., Wang, H. C. and Sun, X. H. (2009) 'Hes1 potentiates T cell lymphomagenesis by up-regulating a subset of notch target genes', *PLoS One* 4(8): e6678.

Duy, C., Yu, J. J., Nahar, R., Swaminathan, S., Kweon, S. M., Polo, J. M., Valls, E., Klemm, L., Shojaee, S., Cerchietti, L. et al. (2010) 'BCL6 is critical for the development of a diverse primary B cell repertoire', *J Exp Med* 207(6): 1209-21.

Falk, I., Nerz, G., Haidl, I., Krotkova, A. and Eichmann, K. (2001) 'Immature thymocytes that fail to express TCRbeta and/or TCRgamma delta proteins die by apoptotic cell death in the CD44(-)CD25(-) (DN4) subset', *Eur J Immunol* 31(11): 3308-17.

Ferreira, A. C., Suriano, G., Mendes, N., Gomes, B., Wen, X., Carneiro, F., Seruca, R. and Machado, J. C. (2012) 'E-cadherin impairment increases cell survival through Notch-dependent upregulation of Bcl-2', *Hum Mol Genet* 21(2): 334-43.

Geimer Le Lay, A. S., Oravecz, A., Mastio, J., Jung, C., Marchal, P., Ebel, C., Dembele, D., Jost, B., Le Gras, S., Thibault, C. et al. (2014) 'The tumor suppressor Ikaros shapes the repertoire of notch target genes in T cells', *Sci Signal* 7(317): ra28.

Goux, D., Coudert, J. D., Maurice, D., Scarpellino, L., Jeannet, G., Piccolo, S., Weston, K., Huelsken, J. and Held, W. (2005) 'Cooperating pre-T-cell receptor and TCF-1-dependent signals ensure thymocyte survival', *Blood* 106(5): 1726-33.

Gutierrez, A. and Look, A. T. (2007) 'NOTCH and PI3K-AKT pathways intertwined', *Cancer Cell* 12(5): 411-3.

Hager-Theodorides, A. L., Furmanski, A. L., Ross, S. E., Outram, S. V., Rowbotham, N. J. and Crompton, T. (2009) 'The Gli3 transcription factor expressed in the thymus stroma controls thymocyte negative selection via Hedgehog-dependent and -independent mechanisms', *J Immunol* 183(5): 3023-32.

Hager-Theodorides, A. L., Rowbotham, N. J., Outram, S. V., Dessens, J. T. and Crompton, T. (2007) 'Beta-selection: abundance of TCRbeta-/gammadelta- CD44-CD25- (DN4) cells in the foetal thymus', *Eur J Immunol* 37(2): 487-500.

Hayday, A. C. and Pennington, D. J. (2007) 'Key factors in the organized chaos of early T cell development', *Nat Immunol* 8(2): 137-44.

Heng, Tracy S. P. and Painter, Michio W. (2008) 'The Immunological Genome Project: networks of gene expression in immune cells', *Nature immunology* 9(10): 1091-4.

Hollister, K., Kusam, S., Wu, H., Clegg, N., Mondal, A., Sawant, D. V. and Dent, A. L. (2013) 'Insights into the role of Bcl6 in follicular Th cells using a new conditional mutant mouse model', *J Immunol* 191(7): 3705-11.

Hong, C., Luckey, M. A. and Park, J. H. (2012) 'Intrathymic IL-7: the where, when, and why of IL-7 signaling during T cell development', *Semin Immunol* 24(3): 151-8.

Hosokawa, H. and Rothenberg, E. V. (2018) 'Cytokines, Transcription Factors, and the Initiation of T-Cell Development', *Cold Spring Harb Perspect Biol* 10(5).

Koch, U. and Radtke, F. (2011) 'Mechanisms of T cell development and transformation', *Annu Rev Cell Dev Biol* 27: 539-62.

Kovall, R. A., Gebelein, B., Sprinzak, D. and Kopan, R. (2017) 'The Canonical Notch Signaling Pathway: Structural and Biochemical Insights into Shape, Sugar, and Force', *Dev Cell* 41(3): 228-241.

LaFoya, B., Munroe, J. A., Mia, M. M., Detweiler, M. A., Crow, J. J., Wood, T., Roth, S., Sharma, B. and Albig, A. R. (2016) 'Notch: A multi-functional integrating system of microenvironmental signals', *Dev Biol* 418(2): 227-41.

Lau, C. I., Barbarulo, A., Solanki, A., Saldana, J. I. and Crompton, T. (2017) 'The kinesin motor protein Kif7 is required for T-cell development and normal MHC

expression on thymic epithelial cells (TEC) in the thymus', *Oncotarget* 8(15): 24163-24176.

Lau, C. I., Outram, S. V., Saldana, J. I., Furmanski, A. L., Dessens, J. T. and Crompton, T. (2012) 'Regulation of murine normal and stress-induced erythropoiesis by Desert Hedgehog', *Blood* 119(20): 4741-51.

Levelt, C. N., Mombaerts, P., Iglesias, A., Tonegawa, S. and Eichmann, K. (1993) 'Restoration of early thymocyte differentiation in T-cell receptor beta-chain-deficient mutant mice by transmembrane signaling through CD3 epsilon', *Proc Natl Acad Sci U S A* 90(23): 11401-5.

Liu, X., Lu, H., Chen, T., Nallaparaju, K. C., Yan, X., Tanaka, S., Ichiyama, K., Zhang, X., Zhang, L., Wen, X. et al. (2016) 'Genome-wide Analysis Identifies Bcl6-Controlled Regulatory Networks during T Follicular Helper Cell Differentiation', *Cell Rep* 14(7): 1735-1747.

Medyouf, H., Gusscott, S., Wang, H., Tseng, J. C., Wai, C., Nemirovsky, O., Trumpp, A., Pflumio, F., Carboni, J., Gottardis, M. et al. (2011) 'High-level IGF1R expression is required for leukemia-initiating cell activity in T-ALL and is supported by Notch signaling', *J Exp Med* 208(9): 1809-22.

Michie, A. M., Chan, A. C., Ciofani, M., Carleton, M., Lefebvre, J. M., He, Y., Allman, D. M., Wiest, D. L., Zuniga-Pflucker, J. C. and Izon, D. J. (2007) 'Constitutive Notch signalling promotes CD4 CD8 thymocyte differentiation in the absence of the pre-TCR complex, by mimicking pre-TCR signals', *Int Immunol* 19(12): 1421-30.

Ono, M., Tanaka, R. J. and Kano, M. (2014) 'Visualisation of the T cell differentiation programme by Canonical Correspondence Analysis of transcriptomes', *BMC Genomics* 15: 1028.

Outram, S. V., Hager-Theodorides, A. L., Shah, D. K., Rowbotham, N. J., Drakopoulou, E., Ross, S. E., Lanske, B., Dessens, J. T. and Crompton, T. (2009) 'Indian hedgehog (Ihh) both promotes and restricts thymocyte differentiation', *Blood* 113(10): 2217-28.

Papaioannou, E., Yanez, D. C., Ross, S., Lau, C. I., Solanki, A., Chawda, M. M., Virasami, A., Ranz, I., Ono, M., O'Shaughnessy, R. F. L. et al. (2019) 'Sonic Hedgehog signaling limits atopic dermatitis via Gli2-driven immune regulation', *J Clin Invest* 129(8): 3153-3170.

Pelullo, M., Quaranta, R., Talora, C., Checquolo, S., Cialfi, S., Felli, M. P., te Kronnie, G., Borga, C., Besharat, Z. M., Palermo, R. et al. (2014) 'Notch3/Jagged1 circuitry reinforces notch signaling and sustains T-ALL', *Neoplasia* 16(12): 1007-17.

Radtke, F., Fasnacht, N. and Macdonald, H. R. (2010) 'Notch signaling in the immune system', *Immunity* 32(1): 14-27.

Rao, S. S., O'Neil, J., Liberator, C. D., Hardwick, J. S., Dai, X., Zhang, T., Tyminski, E., Yuan, J., Kohl, N. E., Richon, V. M. et al. (2009) 'Inhibition of NOTCH signaling by gamma secretase inhibitor engages the RB pathway and elicits cell cycle exit in T-cell acute lymphoblastic leukemia cells', *Cancer Res* 69(7): 3060-8.

Reizis, B. and Leder, P. (2002) 'Direct induction of T lymphocyte-specific gene expression by the mammalian Notch signaling pathway', *Genes Dev* 16(3): 295-300.

Reyes, A., Anders, S., Weatheritt, R. J., Gibson, T. J., Steinmetz, L. M. and Huber, W. (2013) 'Drift and conservation of differential exon usage across tissues in primate species', *Proc Natl Acad Sci U S A* 110(38): 15377-82.

Rowbotham, Nicola J., Hager-Theodorides, Ariadne L., Furmanski, Anna L., Ross, Susan E., Outram, Susan V., Dessens, Johannes T. and Crompton, Tessa (2009) 'Sonic hedgehog negatively regulates pre-TCR-induced differentiation by a Gli2-dependent mechanism', *Blood* 113(21): 5144-56.

Sahni, H., Ross, S., Barbarulo, A., Solanki, A., Lau, C. I., Furmanski, A., Saldana, J. I., Ono, M., Hubank, M., Barenco, M. et al. (2015) 'A genome wide transcriptional model of the complex response to pre-TCR signalling during thymocyte differentiation', *Oncotarget* 6(30): 28646-60.

Sakano, D., Kato, A., Parikh, N., McKnight, K., Terry, D., Stefanovic, B. and Kato, Y. (2010) 'BCL6 canalizes Notch-dependent transcription, excluding Mastermind-like1 from selected target genes during left-right patterning', *Dev Cell* 18(3): 450-62.

Shaffer, A. L., Yu, Xin, He, Yunsheng, Boldrick, Jennifer, Chan, Erick P. and Staudt, Louis M. (2000) 'BCL-6 Represses Genes that Function in Lymphocyte Differentiation, Inflammation, and Cell Cycle Control', *Immunity* 13(2): 199-212.

Shah, D. K. and Zuniga-Pflucker, J. C. (2014) 'An overview of the intrathymic intricacies of T cell development', *J Immunol* 192(9): 4017-23.

Shah, Divya K., Hager-Theodorides, Ariadne L., Outram, Susan V., Ross, Susan E., Varas, Alberto and Crompton, Tessa (2004) 'Reduced thymocyte development in sonic hedgehog knockout embryos', *Journal of immunology (Baltimore, Md. : 1950)* 172(4): 2296-306.

Shin, D. M., Shaffer, D. J., Wang, H., Roopenian, D. C. and Morse, H. C., 3rd (2008) 'NOTCH is part of the transcriptional network regulating cell growth and survival in mouse plasmacytomas', *Cancer Res* 68(22): 9202-11.

Solanki, A., Lau, C. I., Saldana, J. I., Ross, S. and Crompton, T. (2017) 'The transcription factor Gli3 promotes B cell development in fetal liver through repression of Shh', *J Exp Med* 214(7): 2041-2058.

Solanki, A., Yanez, D. C., Ross, S., Lau, C. I., Papaioannou, E., Li, J., Saldana, J. I. and Crompton, T. (2018) 'Gli3 in fetal thymic epithelial cells promotes thymocyte positive selection and differentiation by repression of Shh', *Development* 145(3).

Staal, F. J., Meeldijk, J., Moerer, P., Jay, P., van de Weerdt, B. C., Vainio, S., Nolan, G. P. and Clevers, H. (2001) 'Wnt signaling is required for thymocyte development and activates Tcf-1 mediated transcription', *Eur J Immunol* 31(1): 285-93.

Tzoneva, G. and Ferrando, A. A. (2012) 'Recent advances on NOTCH signaling in T-ALL', *Curr Top Microbiol Immunol* 360: 163-82.

Weng, A. P., Millholland, J. M., Yashiro-Ohtani, Y., Arcangeli, M. L., Lau, A., Wai, C., Del Bianco, C., Rodriguez, C. G., Sai, H., Tobias, J. et al. (2006) 'c-Myc is an important direct target of Notch1 in T-cell acute lymphoblastic leukemia/lymphoma', *Genes Dev* 20(15): 2096-109.

Witkowski, M. T., Cimmino, L., Hu, Y., Trimarchi, T., Tagoh, H., McKenzie, M. D., Best, S. A., Tuohey, L., Willson, T. A., Nutt, S. L. et al. (2015) 'Activated Notch counteracts Ikaros tumor suppression in mouse and human T-cell acute lymphoblastic leukemia', *Leukemia* 29(6): 1301-11.

Wong, G. W., Knowles, G. C., Mak, T. W., Ferrando, A. A. and Zuniga-Pflucker, J. C. (2012) 'HES1 opposes a PTEN-dependent check on survival, differentiation, and proliferation of TCRbeta-selected mouse thymocytes', *Blood* 120(7): 1439-48.

Woolf, E., Xiao, C., Fainaru, O., Lotem, J., Rosen, D., Negreanu, V., Bernstein, Y., Goldenberg, D., Brenner, O., Berke, G. et al. (2003) 'Runx3 and Runx1 are required for CD8 T cell development during thymopoiesis', *Proc Natl Acad Sci U S A* 100(13): 7731-6.

Yanez, D. C., Sahni, H., Ross, S., Solanki, A., Lau, C. I., Papaioannou, E., Barbarulo, A., Powell, R., Lange, U. C., Adams, D. J. et al. (2019) 'IFITM proteins drive type 2 T helper cell differentiation and exacerbate allergic airway inflammation', *Eur J Immunol* 49(1): 66-78.

Yashiro-Ohtani, Yumi, He, Yiping, Ohtani, Takuya, Jones, Mary E., Shestova, Olga, Xu, Lanwei, Fang, Terry C., Chiang, Mark Y., Intlekofer, Andrew M., Blacklow, Stephen C. et al. (2009) 'Pre-TCR signaling inactivates Notch1 transcription by antagonizing E2A', *Genes & development* 23(14): 1665-76.

Ye, B. H., Cattoretti, G., Shen, Q., Zhang, J., Hawe, N., de Waard, R., Leung, C., Nouri-Shirazi, M., Orazi, A., Chaganti, R. S. et al. (1997) 'The BCL-6 proto-oncogene controls germinal-centre formation and Th2-type inflammation', *Nature genetics* 16(2): 161-70.

Yu, Di, Rao, Sudha, Tsai, Louis M., Lee, Sau K., He, Yiqing, Sutcliffe, Elissa L., Srivastava, Monika, Linterman, Michelle, Zheng, Lei, Simpson, Nicholas et al. (2009) 'The transcriptional repressor Bcl-6 directs T follicular helper cell lineage commitment', *Immunity* 31(3): 457-68.

Yu, Q., Erman, B., Park, J. H., Feigenbaum, L. and Singer, A. (2004) 'IL-7 receptor signals inhibit expression of transcription factors TCF-1, LEF-1, and RORgammat: impact on thymocyte development', *J Exp Med* 200(6): 797-803.

Figures
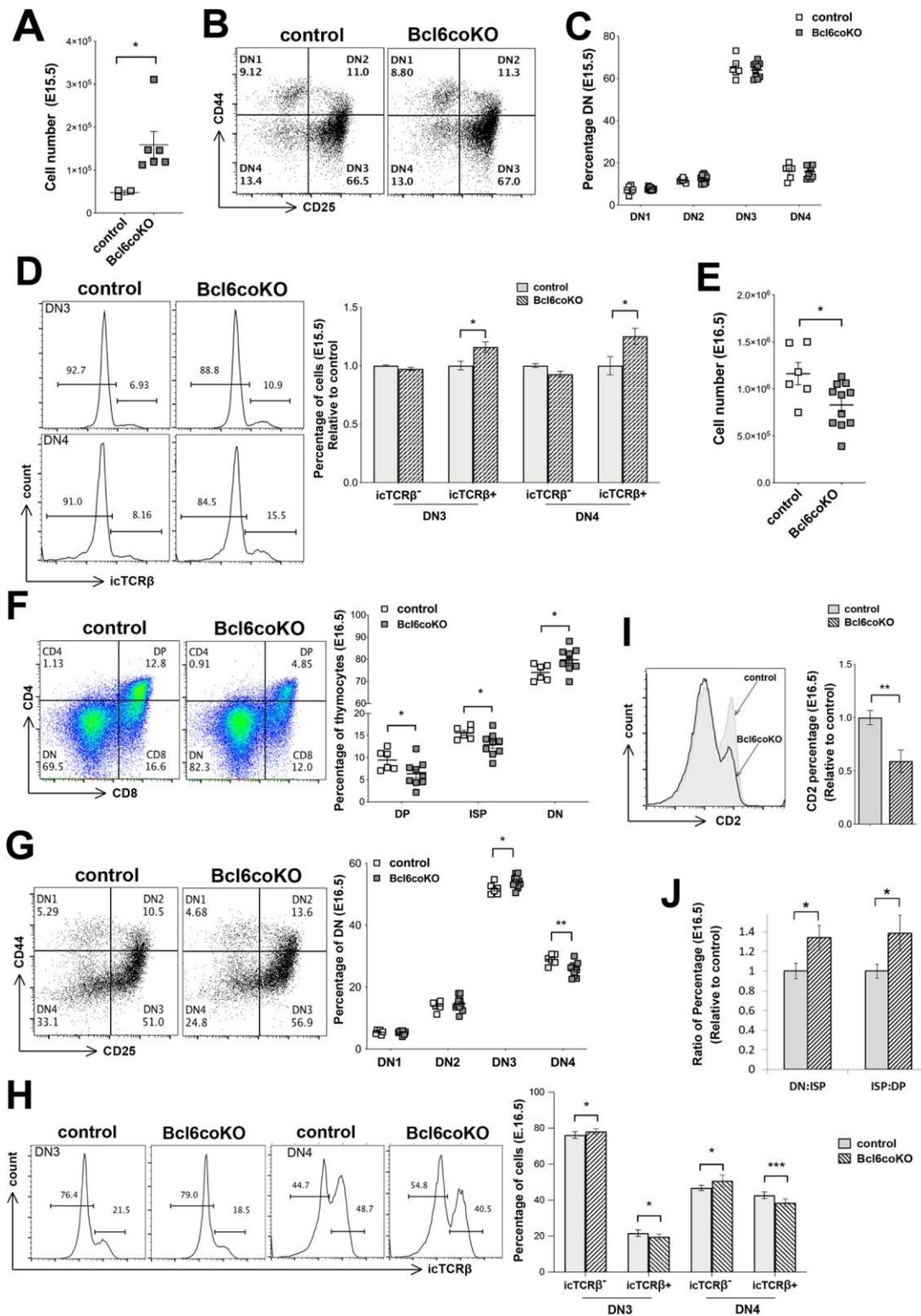
Figure 1: Bcl6 is required for pre-TCR induced differentiation to DP cell in the foetal thymus

(A-D) Thymocyte development in E15.5 Bcl6coKO and littermate embryos (control). (A) Number of thymocytes in E15.5 from control (Cre-; n=3) and Bcl6coKO (n=6) littermate embryos; (p<0.05). (B-C) Analysis of fetal thymus on E15.5 from control (n=6) and Bcl6coKO (n=10). (B) Representative flow cytometry profile of CD44 and CD25 expression, gated on CD3⁻CD4⁻CD8⁻ cells, giving the percentage of cells in the quadrants shown. (C) Scatter plot shows the percentage of double negative (DN1-4) subsets in the control and Bcl6coKO DN population. (D) Histograms show representative intracellular (ic) TCRβ staining in DN3 and DN4 populations, giving the percentage of icTCRβ⁻ and icTCRβ+ cells in the markers shown from E15.5 fetal thymus from control and Bcl6coKO. Bar graph shows the relative percentage of icTCRβ⁻ and icTCRβ+ cells in DN3 and DN4 populations, giving significance by student's t-test in Bcl6coKO compared to control (Cre- littermate) for icTCRβ+ in DN3 population (p<0.05), and icTCRβ+ in DN4 population (p<0.05).

(E-J) Analysis of E16.5 fetal thymus from control (n=6) and Bcl6coKO embryos (n=11). (E) Scatter plot shows number of thymocytes from control and Bcl6coKO (p<0.05). (F) Representative flow cytometry profile of CD4 and CD8 expression, giving the percentage of cells in each quadrant. Scatter plot shows the percentage of different thymocyte populations in control and Bcl6coKO, giving significance for DP (p<0.04); ISP (p<0.05); and DN (p<0.05). (G) Dot plot shows representative profile of CD44 and CD25 expression giving the percentage of cells in each quadrant, gated on CD4⁻CD8⁻ CD3⁻ cells. Scatter plot shows the percentage of the DN1-DN4 subsets in the DN population, giving significance for Bcl6coKO compared to control for DN3 (p=0.03) and DN4 (p=0.007). (H) Representative histograms show icTCRβ expression in DN3 (left

plots) and DN4 (right plots) cells, giving the percentage of cells in the marker shown. Bar chart shows the percentage of icTCRβ⁻ and icTCRβ+ cells in DN3 and DN4 populations, for: icTCRβ⁻ in DN3 ($p<0.05$); icTCRβ+ in DN3 ($p<0.05$); icTCRβ⁻ in DN4 ($p<0.05$); icTCRβ+ in DN4 ($p<0.001$). (I) Representative histogram shows expression of CD2 on E16.5 thymocytes from control and Bcl6coKO thymus . Bar graph shows the relative percentage of CD2+ thymocytes on E16.5 giving significance by student's t-test for Bcl6coKO compared to Cre- littermate ($p<0.01$). (J) Bar chart shows the ratios between different thymocyte populations in control (n=10) and Bcl6coKO (n=8), giving significance by student's t-test for Bcl6coKO compared to Cre- littermate (control) for DN:ISP ($p<0.02$) and ISP:DP ($p<0.04$). Plots show mean ± SEM; in scatter plots each symbol represents an individual embryo.
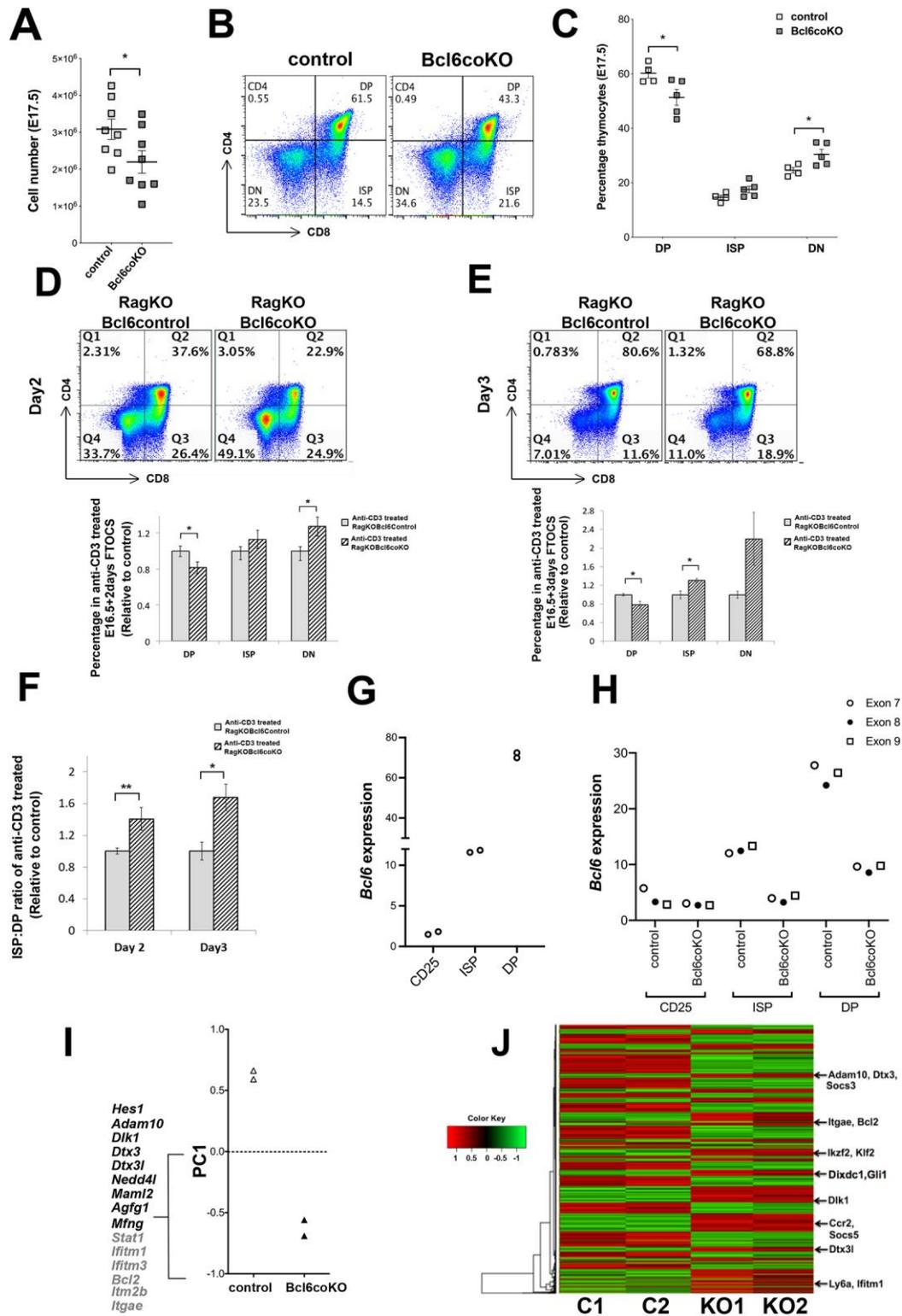
Figure 2: The requirement for Bcl6 at the DN to DP transition is Rag-independent

(A-C) Flow cytometry analysis of E17.5 foetal thymus (A) Scatter plot shows cell number from control (n=8) and Bcl6coKO (n=8) thymus giving significance by student's t-test (p<0.05). (B) Dot plot shows representative CD4 and CD8 expression

giving the percentage of cells in each quadrant, having gated out CD3^{high} cells to exclude γδ T-cells from DN and ISP. (C) Scatter plot shows the percentage of different thymocyte populations, giving significance for DP (p<0.05) and DN (p<0.05) for control (n=4) and Bcl6coKO embryos (n=5).

(D-F) Flow cytometry analyses of thymocyte populations in E16.5 RagKOBcl6coKO and RagKOBcl6control FTOC treated with anti-CD3 for (D) 2 days and (E) for 3 days. The number of cells recovered from each FTOC was not significantly different between genotypes on day 2 or day 3. (D) Upper: representative flow cytometry profile of CD4 and CD8 expression, giving the percentage of cells in each quadrant. Lower: bar chart shows the relative percentage of thymocyte populations, giving significance by student's t-test compared to RagKOBcl6control littermate for DP (p<0.05) and DN (p<0.05), for RagKOBcl6control (n=15) and RagKOBcl6coKO (n=10). (E) Upper: representative flow cytometry profile of CD4 and CD8 expression. Lower: bar graph shows relative percentage of thymocyte populations, giving significance by student's t-test compared to RagKOBcl6control (n=4) relative to control littermate (n=3) for DP (p<0.05) and ISP (p<0.05). (F) Bar graph showing relative ratio of ISP:DP on day 2 and day 3 of anti-CD3 treated FTOC for RagKOBcl6coKO, giving significance by student's t-test compared to RagKOBcl6control littermate for ISP:DP (2 day-treated: p<0.01; 3 day-treated: p<0.05). (G) *Bcl6* expression by RNA-sequencing expressed as RPKM (reads per kilobase of transcript per million mapped reads) from facs-sorted CD25+DN from untreated E16.5 RagKOBcl6control (Cre-) FTOC, and from ISP and DP populations from anti-CD3-treated E16.5 RagKOBcl6control (Cre-) FTOC after 2 days in culture (n=2). (H) Mean expression (normalised reads) of exons 7 (open circles), 8 (filled circles) and 9 (squares) of *Bcl6* in facs-sorted CD25+DN from untreated E16.5 RagKOBcl6coKO (Bcl6coKO) and RagKOBcl6control (Cre-) (control) FTOC, and
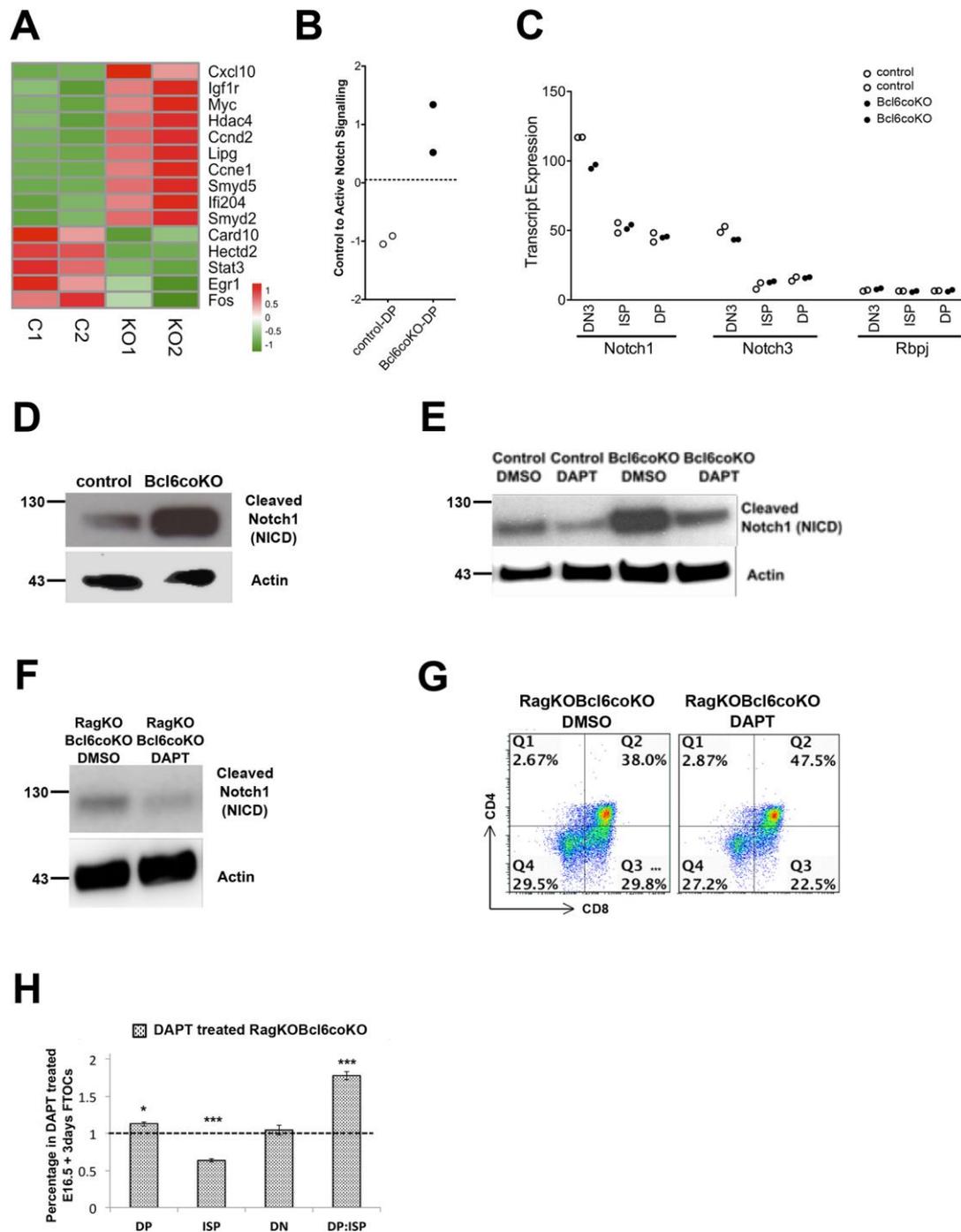
from ISP and DP populations from anti-CD3-treated E16.5 RagKOBcl6coKO and RagKOBcl6control (Cre-) FTOC after 2 days in culture (n=2). (I) Principal Component Analysis (PCA) of whole transcriptome RNA-sequencing datasets from purified CD25+DN thymocytes from E16.5 untreated RagKOBcl6control (n=2, open triangles) and RagKOBcl6coKO (n=2, filled triangles) separates datasets by genotype on PC1. Bcl6 target genes (shown in grey) and Notch signalling and target genes (shown in black) contribute to the negative access of PC1 (more highly expressed in the Bcl6coKO datasets compared to control). (J) Heat map shows the intersection of the 3000 genes that contributed most to PC1 with 1500 significant DEG (p<0.05) between RagKOBcl6control (C1 and C2) and RagKOBcl6coKO (KO1 and KO2) CD25+DN datasets. Normalized expression values are represented as a z score where green is lower expression and red is higher expression (see colour key). Plots show mean ± SEM; in scatter plots in A and C each symbol represents an individual embryo.
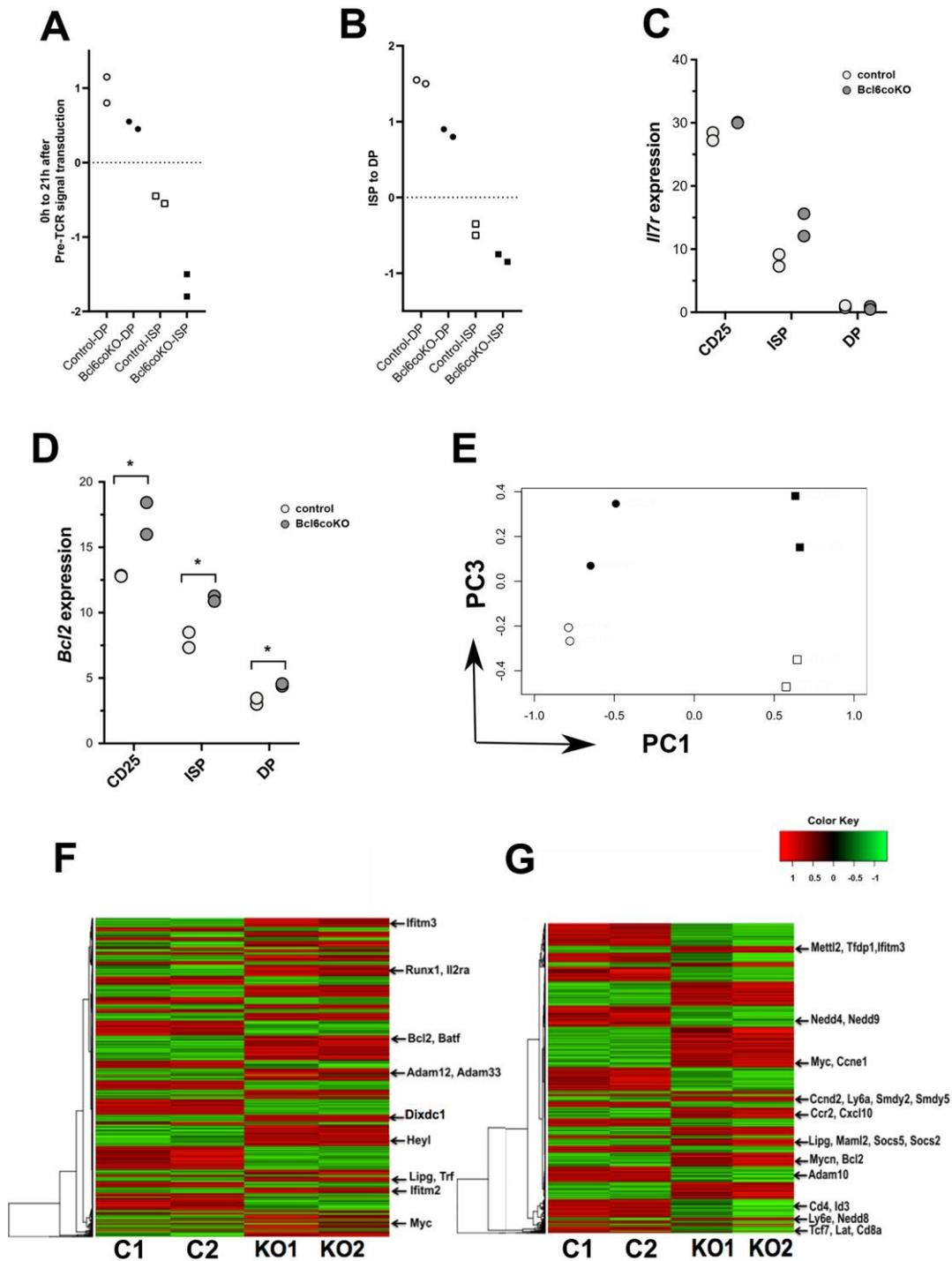
Figure 3: Conditional deletion of *Bcl6* influences maturation and Notch associated genes

(A-G) Whole transcriptome RNA-sequencing datasets from facs-sorted DP and ISP thymocyte populations from anti-CD3-treated E16.5 RagKOBcl6control (n=2) and RagKOBcl6coKO (n=2) FTOC after 2 days. (A) Canonical Correspondence Analysis

(CCA) using pre-TCR timecourse data (E-MTAB-3088) shows that DP (circles) and ISP (squares) datasets of RagKOBcl6coKO (solid shapes) have a transcriptional signature of slower differentiation compared to their control (open shapes) counterparts. (B) CCA using Immgen Datasets DP and ISP from Immgen (GSE15907) shows that both DP (circles) and ISP (squares) datasets of RagKOBcl6coKO (solid shapes) have the transcriptional signature of less mature thymocytes than their control (open shapes) counterparts. (C-D) *Il7r* (C) and *Bcl2* (D) expression by RNA-sequencing expressed as RPKM (reads per kilobase of transcript per million mapped reads) from facs-sorted CD25+DN (CD25, n=2) from untreated RagKOBcl6control (Cre-) and RagKOBcl6coKO, and from ISP and DP populations from anti-CD3-treated E16.5 RagKOBcl6control (Cre-) and RagKOBcl6coKO FTOC after 2 days in culture (n=2). The differences in expression between genotypes for each facs-sorted population were not statistically significant by EBayes statistics for *Il7r* (C) but were significant for *Bcl2* (D) ($p<0.05$). (E) PCA showing separation of ISP (squares) from DP (circles) datasets on PC1 and separation of RagKOBcl6control (open shapes) from RagKOBcl6coKO (solid shapes) for both ISP and DP datasets on PC3. (F) Heatmap showing DEG ($p<0.05$) for ISP datasets for RagKOBcl6control (C1, C2) and RagKOBcl6coKO (KO1, KO2), selected by intersection of 4000 genes that contributed most to PC3 with 1800 DEG ($p<0.05$). Normalized expression signals are represented as a z score where green represents lower expression and red higher expression levels (see colour key). (G) Heatmap showing DEG ($p<0.05$) for DP datasets for RagKOBcl6control (C1, C2) and RagKOBcl6coKO (KO1, KO2), selected by intersection of 4000 genes that contributed most to PC3 with 3100 significant DEG ($p<0.05$). Normalized expression scores are represented as a z score where green represents lower expression and red higher expression levels (see colour key).
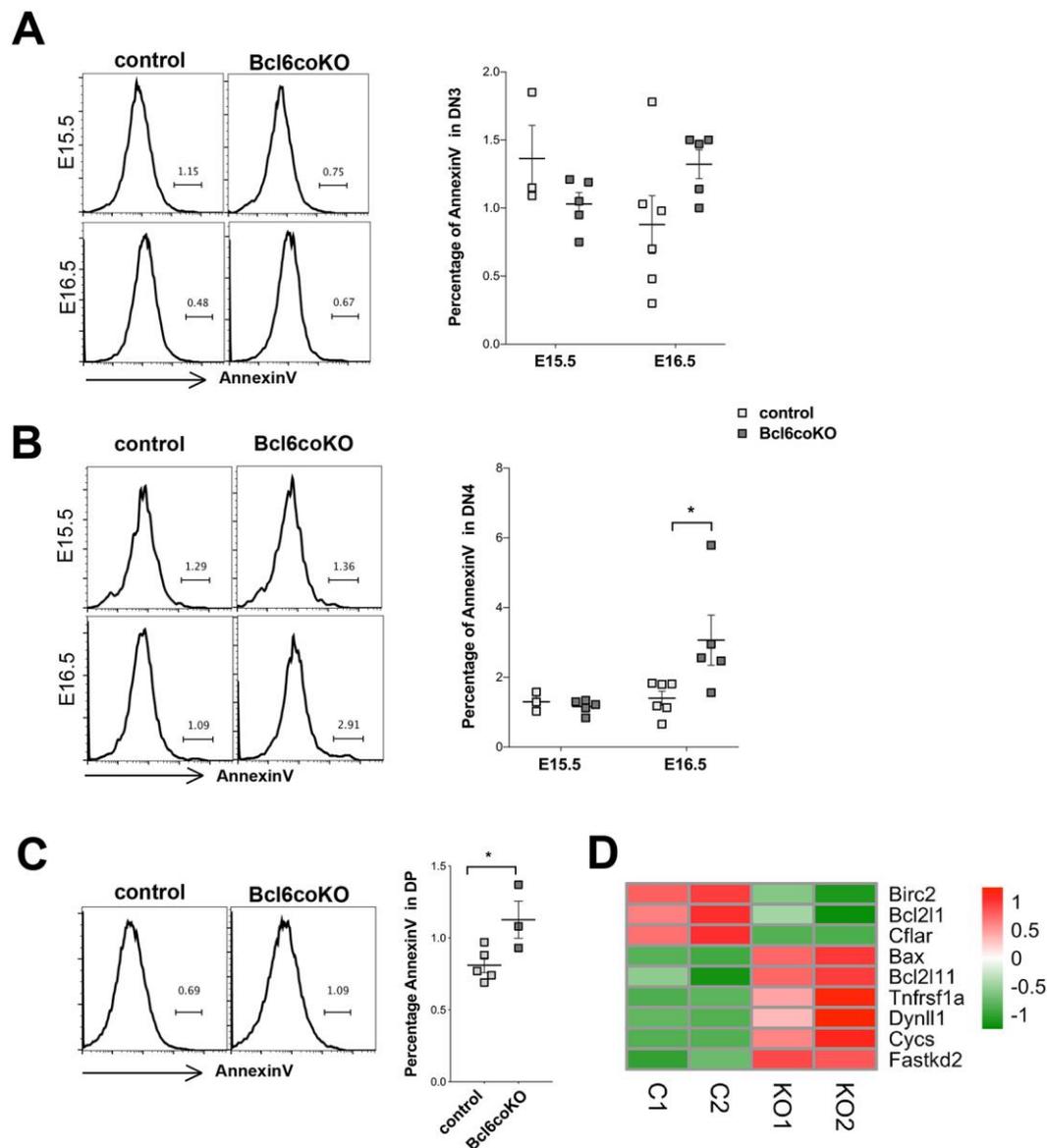
Figure 4: Conditional deletion of Bcl6 increases Notch-mediated transcription and NICD in developing thymocytes.

(A-C) Analysis of RNA-sequencing datasets from E16.5 facs-sorted CD25+DN from untreated E16.5 RagKOBcl6control (Cre-) and RagKOBcl6coKO FTOC, and from ISP and DP populations from anti-CD3-treated E16.5 RagKOBcl6control (Cre-) and RagKOBcl6coKO FTOC after 2 days in culture (n=2). (A) Pearson correlation heat

map shows normalized expression of several DEG known to be up-regulated (*Cxcl10,*
Igfr1, Myc, Hdac4, Ccnd2, Lipg, Ccne1, Smyd5, Ifi204, Smyd2) and down-regulated
(*Card10, Hectd2, Stat3, Egr1, Fos*) by Notch1 activation in thymocytes, represented as
a z score where green is lower expression and red is higher expression levels (see colour
key) on a linear scale in DP datasets from RagKOBcl6control (C1, C2) and
RagKOBcl6coKO (KO1, KO2) datasets. (B) CCA was used to generate a scale of
control to active Notch1 signalling, using publicly available transcriptome datasets from
thymocytes with normal levels and high levels of Notch signalling from GSE67572,
showing that RagKOBcl6coKO (solid circles) DP datasets have a transcriptional
signature of increased Notch-mediated transcription compared to RagKOBcl6control
(open circles) DP datasets. (C) Scatter plot shows expression (RPKM, reads per kilobase
of transcript per million mapped reads) of *Notch1*, *Notch3* and *Rbpj* in CD25+DN, from
untreated E16.5 RagKOBcl6coKO (solid circles) and RagKOBcl6control (open circles)
and from ISP and DP populations from anti-CD3 treated E16.5 RagKOBcl6coKO (solid
circles) and RagKOBcl6control (open circles) FTOC. (D) Western blot showing the
expression of activated Notch1 protein (NICD) in E16.5 control (Cre-) and Bcl6coKO
thymocytes (upper panel). Lower panel shows Actin as loading control. Quantification
of bands and normalisation relative to Actin revealed a ~2.76 fold increase in NICD
expression in the Bcl6coKO thymocytes compared to control. (E) Western blot shows
expression of NICD protein in E16.5 control (Cre-) and Bcl6coKO FTOC after 2 days
treatment with DAPT(1μM) or its vehicle (DMSO) (upper panel). Lower panel shows
Actin as loading control. Quantification of bands and normalisation relative to Actin
revealed that NICD was reduced following DAPT treatment in both the control and
Bcl6coKO thymocytes compared to their respective DMSO controls by ~two-fold. (F)
Western blot showing the expression of activated Notch1 protein (NICD) in anti-CD3-

treated RagKOBcl6coKO E16.5 FTOCs, treated with DAPT (1μM) or its vehicle (DMSO) control (upper panel) for 2 days. Lower panel shows Actin as loading control. Quantification of bands and normalisation relative to Actin revealed that NICD expression following DAPT (1μM) treatment was reduced ~two-fold compared to DMSO control. (G-H) Flow cytometry analysis of FTOC after 3 days anti-CD3 treatment in DAPT-treated RagKOBcl6CoKO (n=4) compared to DMSO-treated (control) RagKOBcl6CoKO (n=4). (G) Representative flow cytometry profile of CD4 and CD8 expression. (H) Bar graph shows relative percentage of thymocyte populations in DMSO-treated FTOC and ratio of DP:ISP giving significance by student's t-test for DP (p<0.05), ISP (p<0.001), DN and DP:ISP (p<0.001), compared to DMSO control. In Western blots horizontal black lines show position of molecular weight markers (kDa).

Figure 5: Conditional deletion of Bcl6 increases cell death in foetal DN thymocytes

(A-B) Flow cytometry analysis of AnnexinV staining in foetal DN thymocyte populations (gated on CD3⁻CD4⁻CD8⁻CD44⁻) from control and Bcl6coKO. (A) Histograms (left) show representative AnnexinV staining cells in the DN3 population on E15.5 (upper panel) and E16.5 (lower panel), giving the percentage of cells in the marker shown. Scatter plot (right) shows the percentages of AnnexinV+ cells in the DN3 populations. (B) Histograms (left) show representative AnnexinV staining cells in the DN4 population on E15.5 (upper) and E16.5 (lower). Scatter plot (right) shows the percentages of AnnexinV+ cells in the DN4 populations, giving significance for E16.5

(p<0.05). (C) Histograms show representative AnnexinV staining in foetal DP population. Scatter plot (right) shows the percentages of AnnexinV+ cells in the DP populations, giving significance (p<0.05). (D) Pearson correlation heatmap showing DEG (p<0.05) for DP datasets from E16.5 RagKOBcl6control (C1 and C2) and RagKOBcl6coKO (KO1 and KO2) FTOC treated with anti-CD3-treated for 2 days, showing some survival (*Cflar*, *Birc2* and *Bcl2l1)* and pro-apoptotic (*Fastkd2*, *Bax*, *Cycs*, *Bcl2l11*, *Tnfrsf1a*, *Dynll1)* genes. Normalized expression values are represented on a linear scale where green is lower expression and red higher expression levels (see colour key).

Plots show mean ± SEM; in scatter plots each symbol represents an individual embryo.
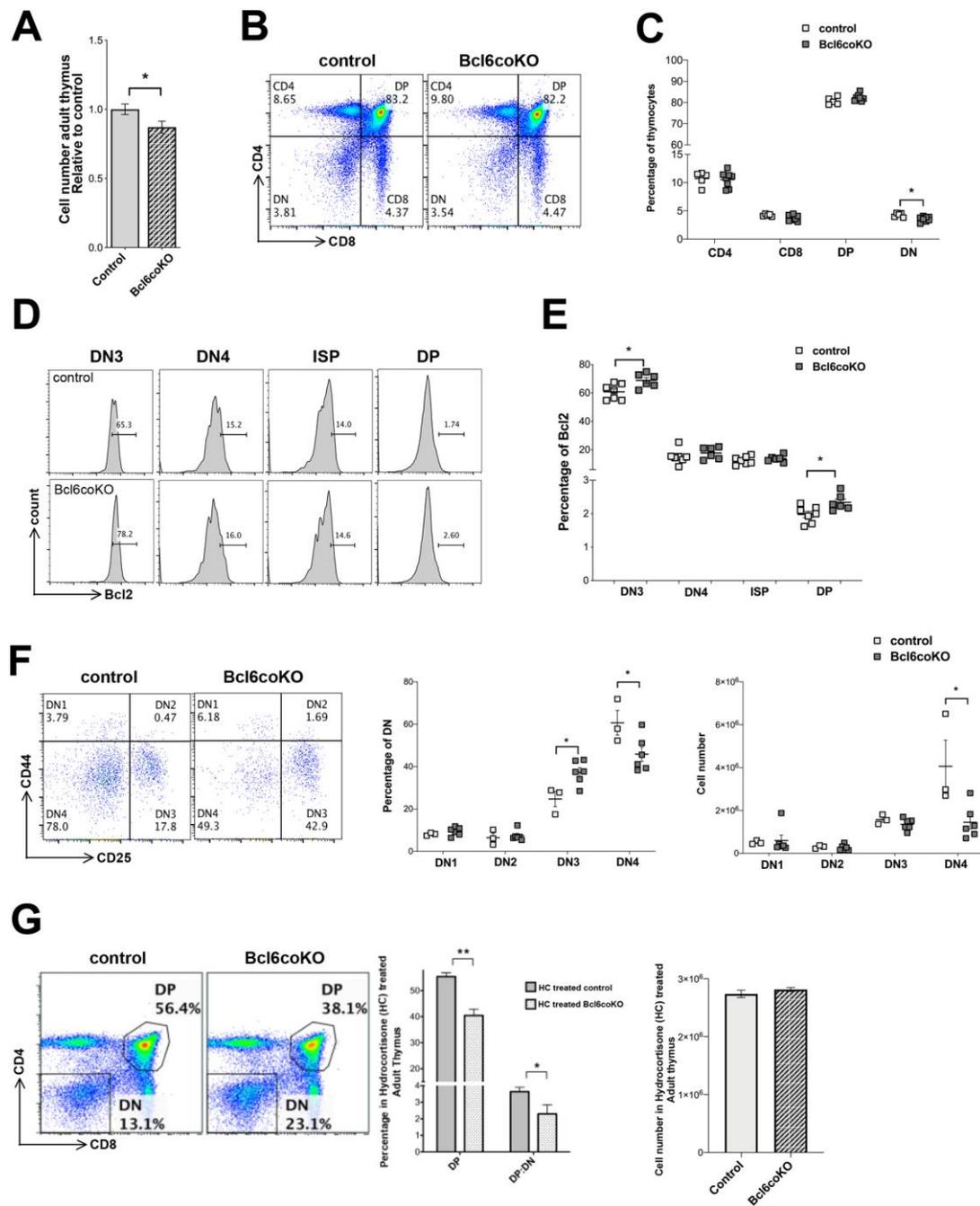
Figure 6: Bcl6 promotes the transition from DN3 to DP cell in the adult thymus

Flow cytometry analysis of adult thymus from control and Bcl6coKO mice. (A) Bar graph shows the relative cell number of control (n=10) and Bcl6coKO (n=13) adult littermate thymus pooled from 3 experiments, giving significance by student's t-test compared to control littermate (p<0.05). (B) Representative flow cytometry profile of CD4 and CD8 expression, giving the percentage of cells in each quadrant for control and Bcl6coKO thymus. (C) Scatter plot shows the percentage of different thymocyte

populations in control (n=6) and Bcl6coKO (n=7), giving significance for DN (p<0.05). (D-E) Flow cytometry analysis of intracellular Bcl2 expression in thymocyte populations. (D) Histograms show representative intracellular anti-Bcl2 staining gated on DN3 (CD3-CD44-CD25+CD4-CD8-), DN4 (CD3-CD44-CD25-CD4-CD8-), ISP (CD3-CD4-CD8+) and DP (CD4+CD8+) populations from control and Bcl6coKO thymus, giving the percentage of cells in the marker shown. (E) Scatter plot shows percentages of positive cells in the different thymocyte subsets from control (n=7) and Bcl6coKO (n=6), giving significance for DN3 (p<0.05) and DP (p<0.05). Each point represents an individual mouse. (F) Left: Representative flow cytometry profile of CD44 and CD25 expression, gated on CD4$^-$CD8$^-$CD3$^-$ cells, giving the percentage of cells in each quadrant. Middle: Scatter plot shows the percentage of the DN subsets (DN1-4) within the CD4$^-$CD8$^-$CD3$^-$ DN population, from control (n=3) and Bcl6coKO (n=6) giving significance for DN3 (p<0.05) and DN4 (p<0.05). Right: scatter plot shows the number of cells in each DN subset for control (n=3) and Bcl6coKO (n=6) thymus, giving significance for DN4 (p<0.05). (G) Flow cytometry analysis of adult thymus 3 days after hydrocortisone (HC) treatment. Representative flow cytometry profile (left panel) of CD4 and CD8 expression, giving the percentage of DN and DP cells in the regions shown for control (left) and Bcl6coKO (right). Bar graph (middle panel) shows the percentage of DP cells and the DP:DN ratio in Bcl6coKO adult thymus (n=3), giving significance by student's t-test compared to control (Cre-) adult thymus, for DP (p<0.01) and DP:DN ratio (p<0.05). Bar chart (right panel) shows the number of cells recovered from control and Bcl6coKO thymus. Plots show mean ± SEM; in scatter plots each symbol represents an individual mouse.
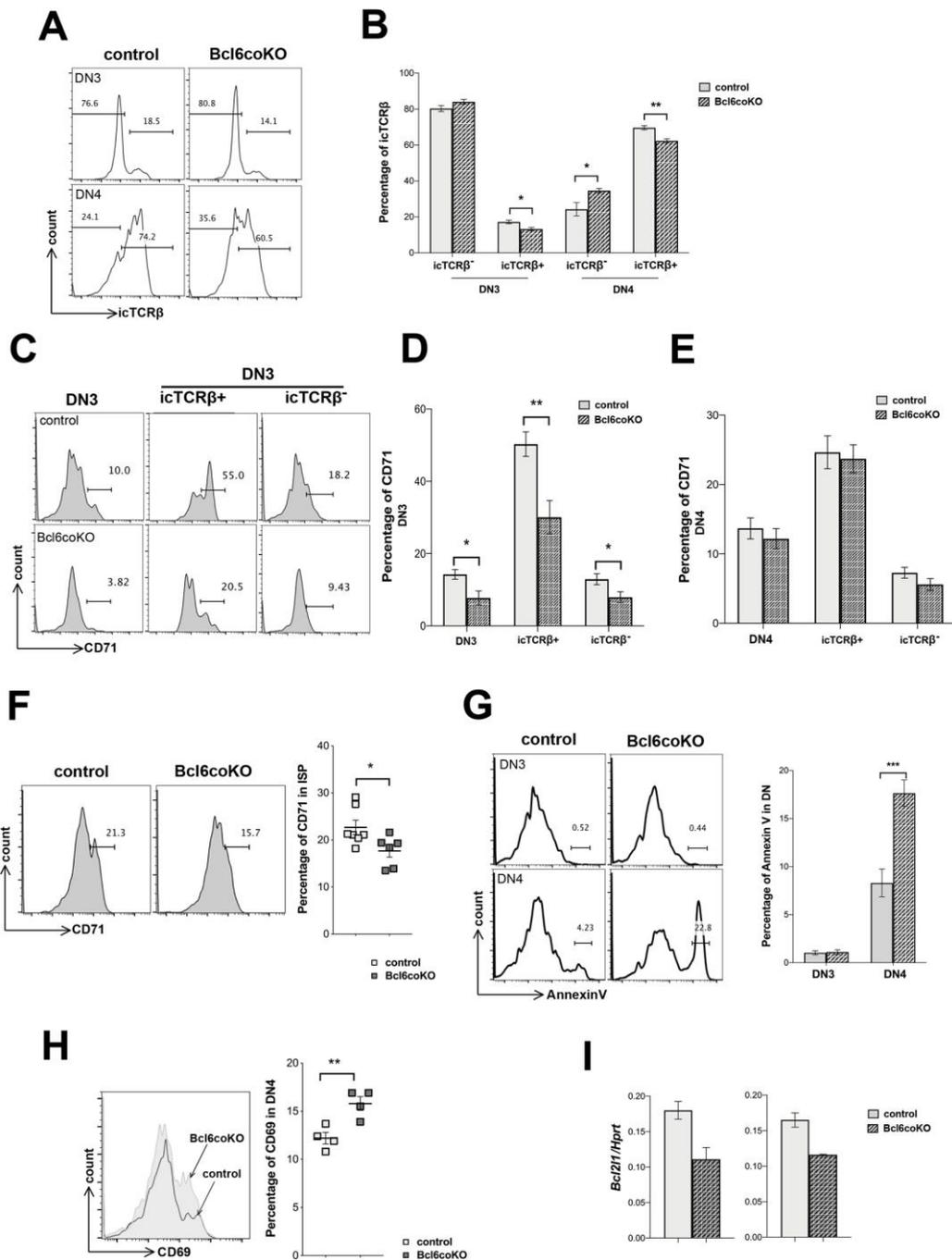
Figure 7: Bcl6 is required for enrichment of icTCRβ+ DN cells and DN4 survival in the adult thymus

Analysis of DN subsets in adult thymus from control and Bcl6coKO mice. (A) Representative histograms show intracellular (ic)TCRβ expression in DN3 (upper) and DN4 (lower) populations in adult Bcl6coKO and control littermate thymus, giving the percentage of cells in the markers shown. (B) Bar graph shows percentage of icTCRβ+

and icTCRβ⁻ cells in DN3 and DN4 populations, giving significance for: icTCRβ+ in DN3 (p<0.05); icTCRβ⁻ in DN4 (p<0.05); icTCRβ+ in DN4 (p<0.01); control n=7, Bcl6coKO n=6. (C) Representative CD71 expression in DN3, icTCRβ+ DN3 and icTCRβ⁻DN3 populations from control (upper) and Bcl6coKO (lower), giving the percentage of positive cells in the marker shown. (D) Barchart shows the percentage of CD71+ cells in DN3, icTCRβ+ DN3 (TCRβ+) and icTCRβ⁻DN3 (TCRβ⁻) populations, giving significance for: DN3 (p<0.05); icTCRβ+ DN3 (p<0.01); icTCRβ⁻DN3 (p<0.05); control n=7; Bcl6coKO n=6. (E) Bar chart shows the percentage of CD71+ cells in DN4, icTCRβ+ DN4 (TCRβ+) and icTCRβ⁻DN4 (TCRβ⁻) populations; control n=7; Bcl6coKO n=6. (F) Representative histograms show flow cytometry analysis of CD71 expression on control and Bcl6coKO ISP (CD8+CD4⁻CD3⁻), giving the percentage of cells in the marker shown. Scatter pot (right) shows the percentage of CD71+ cells in the ISP population for control (n=7) and Bcl6coKO (n=6), giving significance (p<0.05). (G) Histograms (left) show AnnexinV staining in DN3 (upper panels) and DN4 (lower panels), giving the percentage of cells in the markers shown. Bar chart (right) shows the percentage of AnnexinV+ cells in the DN3 and DN4 populations, giving significance for DN4 (p<0.001); control n=7; Bcl6coKO n=9. (H) Representative histograms show flow cytometry analysis of CD69 expression in DN4 populations from control (black line) and Bcl6coKO (grey filled). Scatter plot (left) shows the percentages of CD69+ cells in the DN4 population from control (n=4) and Bcl6coKO (n=4), giving significance (p<0.01). (I) Bar graphs show QRT-PCR for expression of *Bcl2l1* relative to *Hprt* expression in facs-sorted DN4 thymocytes from control and Bcl6coKO. Each plot shows a different experiment from separate facs-sorts from different mice (biological replicates). Plots show mean ± SEM; in scatter plots each symbol represents an individual mouse.

Supplementary Fig.1

A
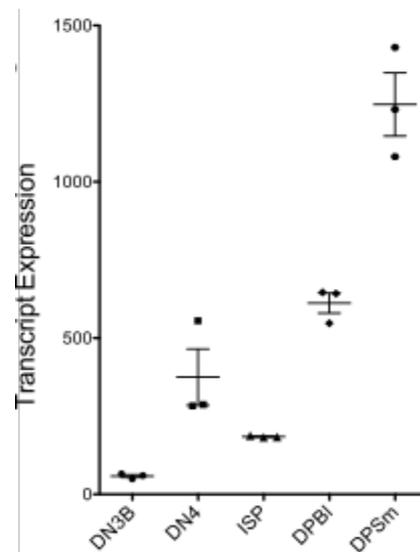
B
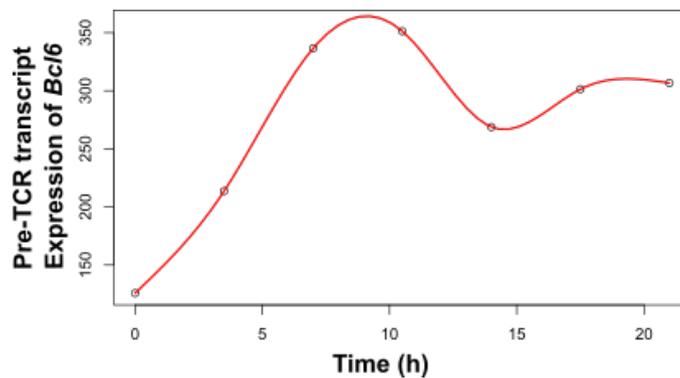
Figure S1 (Figure S1): *Bcl6* **is upregulated following pre-TCR signal transduction and regulates foetal thymocyte development on E15.5**

(A) *Bcl6* transcript expression in sorted thymocyte populations from the Immgen database (GSE15907): DN3B, DN4, ISP DPblast (DPBl) and DPsmall (DPSm).

(B) Transcript expression of *Bcl6* in anti-CD3 treated Rag1-/- thymocytes plotted against time (hours), where t=0 is when the stimulus was added in FTOC, determined by microarray (E-MTAB-3088).
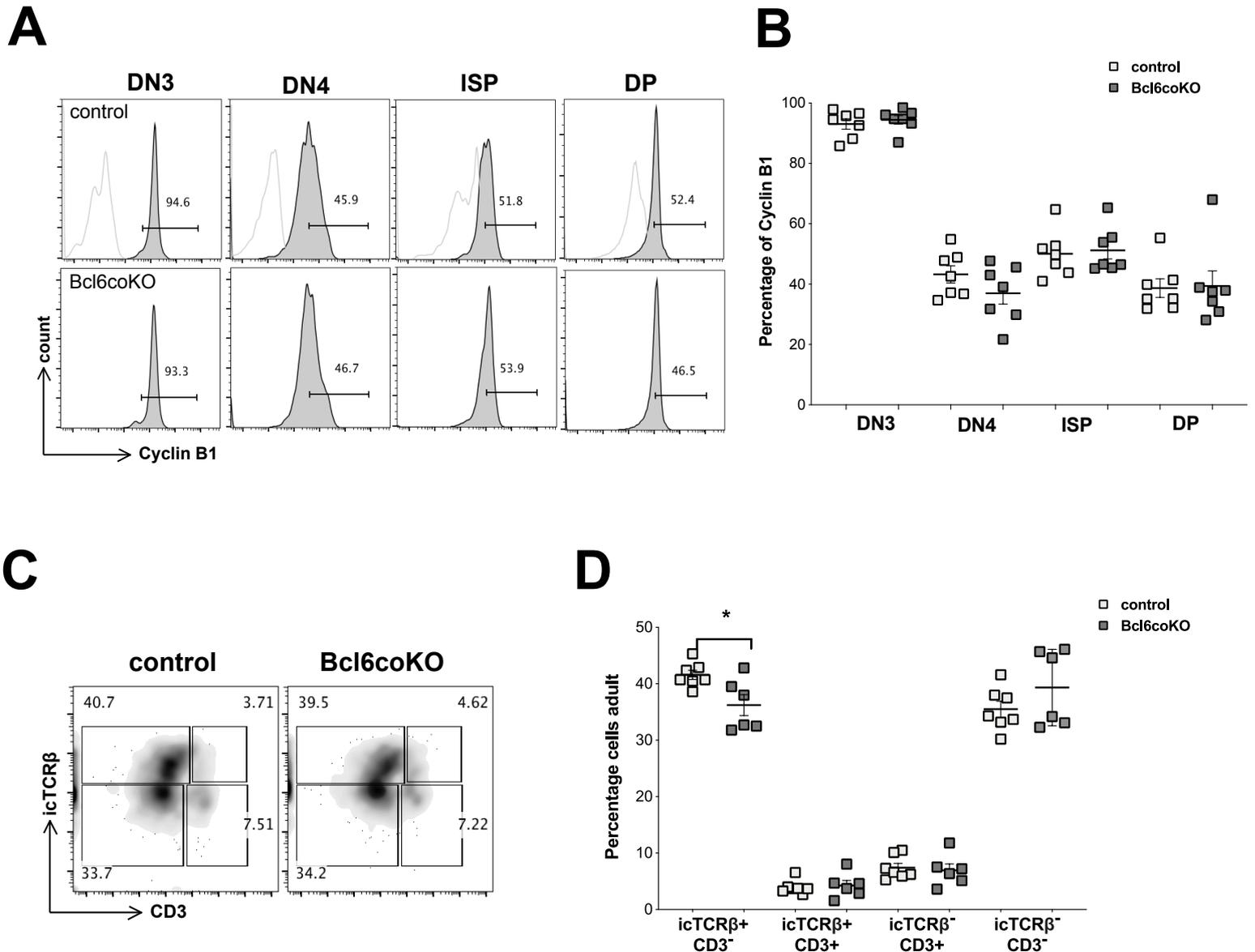
Supplementary Fig.2

A

B

C

D
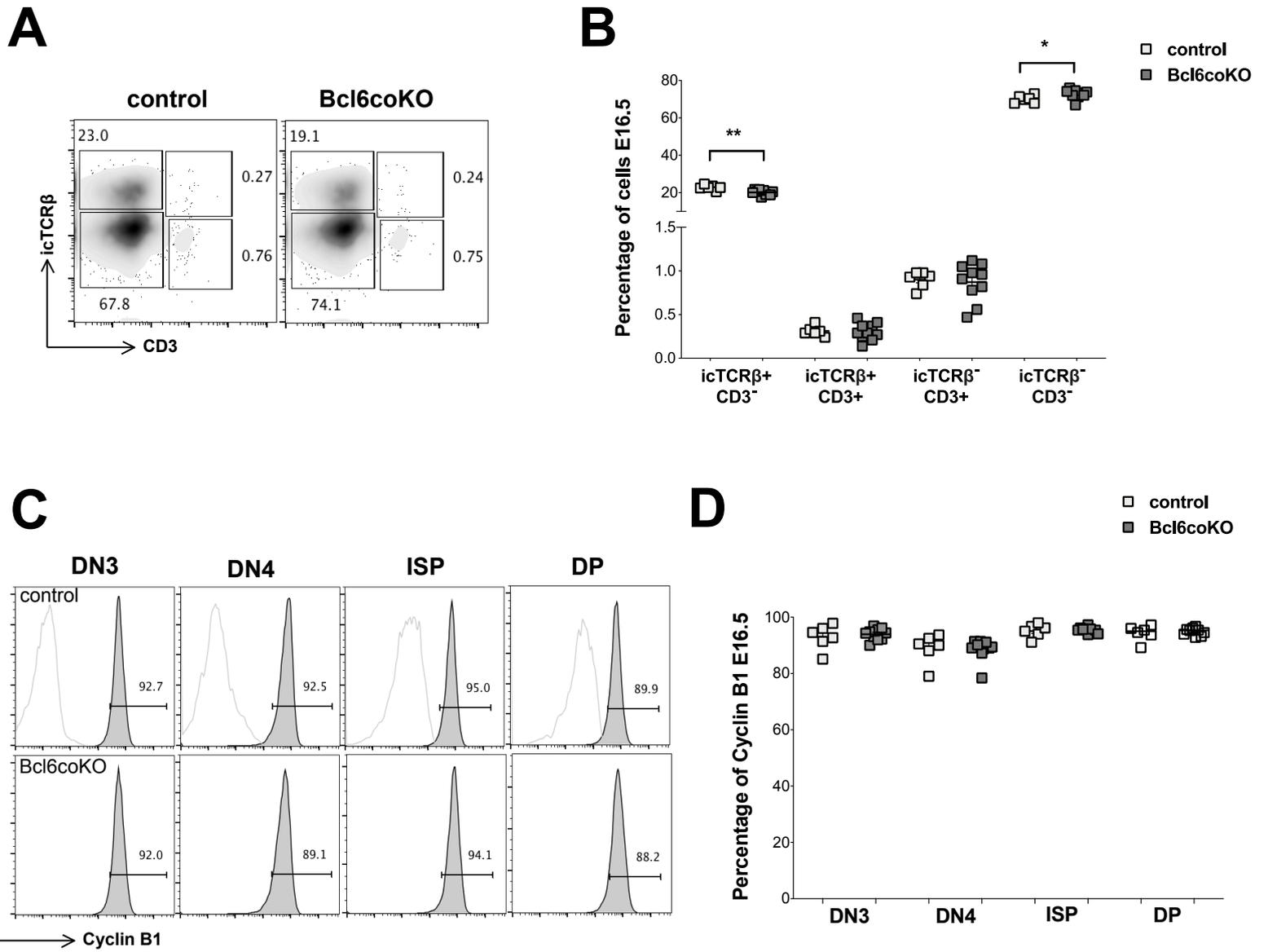
Figure S2 (Figure S2): CD3+TCRβ- cells (γδ T-cells) and intracellular Cyclin B1 expression in E16.5 Bcl6coKO and control thymus

(A-B) Flow cytometry analysis of icTCRβ and cell surface CD3 expression gated on DN cells (CD4-CD8-). (A) Density plots show representative staining of E16.5 foetal thymus from control and Bcl6coKO, giving percentage of cells in the regions shown. (B) Scatter plot shows percentages of cells from control (n=6, light squares) and Bcl6coKO (n=10, dark squares) thymus giving significance by student's t-test for icTCRβ+CD3- ($p<0.05$) and icTCRβ-CD3- ($p=0.05$), where each point represents an individual embryo. There was no significant difference in the proportion of icTCRβ-CD3+ cells which represent the γδ T-cell population between control and Bcl6coKO.

(C-D) Flow cytometry analysis of intracellular Cyclin B1 expression in E16.5 thymocyte populations. (C) Histograms shows representative intracellular anti-Cyclin B1 staining gated on DN3 (CD3-CD44-CD25+), DN4 (CD3-CD44-CD25-) and ISP (CD3-CD4-CD8+) and DP (CD4+CD8+) populations in E16.5 foetal thymus from control and Bcl6coKO, giving the percentage of cells in the marker shown, and the negative control (isotype-matched) staining as a faint overlay. (D) Scatter plot shows percentages of cells in the different thymocyte subsets from control (n=6, light squares) and Bcl6coKO (n=10, dark squares) thymus, where each point represents an individual embryo.

Supplementary Fig.3

A

B

C

D

Figure S3 (Figure S3):   Intracellular Cyclin B1 expression and CD3+TCRβ-cells (γδ T-cells) and in adult Bcl6coKO and control thymus

(A-B) Flow cytometry analysis of intracellular Cyclin B1 expression in adult thymocyte populations. (A) Histograms shows representative intracellular anti-Cyclin B1 staining gated on DN3 (CD3-CD44-CD25+CD4-CD8-), DN4 (CD3-CD44-CD25-CD4-CD8-) and ISP

(CD3-CD4-CD8+) and DP (CD4+CD8+) populations in adult thymus from control and Bcl6coKO, giving the percentage of cells in the marker shown, and the negative control (isotype-matched) staining as a faint overlay. (B) Scatter plot shows percentages of cells in the different thymocyte subsets from control (n=7, light squares) and Bcl6coKO (n=7, dark squares) thymus, where each point represents an individual mouse.

(C-D) Flow cytometry analysis of icTCRβ and cell surface CD3 expression gated on DN cells (CD4-CD8-). (C) Density plots show representative staining, giving the percentage of cells in the regions shown. (D) Scatter plot shows percentages of cells from control (n=6, light squares) and Bcl6coKO (n=10, dark squares) thymus giving significance by student's t-test for icTCRβ+CD3- ($p < 0.05$), where each point represents an individual embryo. There was no significant difference in the proportion of icTCRβ-CD3+ cells which represent the γδ T-cell population between control and Bcl6coKO.

Table S1: Relating to Materials and Methods

Click here to Download Table S1